CHALMERS

Reduction Index Modeling by Finite Elements

Applied on a Double Leaf Construction

Master's Thesis in the Master's programme in Sound and Vibration

MORTEN LINDBORG

Department of Civil and Environmental Engineering
Division of Applied Acoustics
Vibroacoustics Group
CHALMERS UNIVERSITY OF TECHNOLOGY
Göteborg, Sweden 2005

Master's Thesis 2005:55

MASTER'S THESIS 2005:55

Reduction Index Modeling by Finite Elements

- Applied on a Double Leaf Construction

Master's Thesis in the Master's programme in Sound and Vibration

MORTEN LINDBORG

Department of Civil and Environmental Engineering
Division of Applied Acoustics
Vibroacoustics Group
CHALMERS UNIVERSITY OF TECHNOLOGY
Göteborg, Sweden 2005

Reduction Index Modeling by Finite Elements
- Applied on a Double Leaf Construction

Master's Thesis 2005:55

Department of Civil and Environmental Engineering
Division of Applied Acoustics
Vibroacoustics Group
Chalmers University of Technology
SE-41296 Göteborg
Sweden

Tel. +46-(0)31 772 1000

Cover:
Displacement of the plates in a double leaf construction when a plane sound wave at 2000 Hertz, hits from above at an incident angle of 45 degrees.

Reproservice / Department of Civil and Environmental Engineering
Göteborg, Sweden 2005

Reduction Index Modeling by Finite Elements
- Applied on a double leaf construction

MORTEN LINDBORG
Department of Civil and Environmental Engineering
Division of Applied Acoustics
Vibroacoustics Group
Chalmers University of Technology

Abstract

When a sound is traveling from one room to another through a wall, it changes character. In most cases the wanted change is to reduce the level of the sound and, different walls do that differently well. A measure of how much the sound is lowered in level is the so-called *reduction index*, which is dependent on the material properties and geometry of the separating structure, (i.e. the wall).

The aim of this work has been to investigate the possibility to construct a computer model for calculating the reduction index of a structure. The finite element method has been used to investigate the vibrations in a structure cased by air-borne sound waves. The vibrations propagate through the structure leading to a radiation of sound on the opposite side. The difference in sound pressure level on both sides of the structure determines the value of the reduction index for the specific structure.

When a 2D finite element model was developed, a parameter study was performed where the material properties of the structure was changed in a controlled manner. Conclusions of the results from the parameter study was drawn, both to get a confirmation of the model and the influence material properties have on the reduction index.

The results from the model agreed well with earlier calculation methods for double walls. Therefore, the model is expected to deliver good results also for more complex structures.

The parameter study show some interesting results when looking at two differently stiff plates coupled to each by air and studs. At some frequencies the reduction index is dependent of in which direction the sound is traveling through the structure. If the sound hits the stiffer plate first, a higher reduction index can be seen than if the sound hits the softer plate and is radiated from the stiff plate.

Key words: Reduction index, double leaf wall, finite element, modeling, building acoustics

Acknowledgements

First of all I want to mention my grandmother, Vera Møller who is not easily fooled when it comes to science. That is because she immediately takes the position that a new discovery is not true. It takes some effort and explanation to convince her. I have developed a patience and, therefore; also the ability to teach my old grandmother some things about science. So, hopefully some of my patience is reflected on you, when trying to read this report.

I want to thank my supervisor, Krister Larsson and my examiner, Wolfgang Kropp for helping me with defining the problem and a way to handle the calculations. Also all the people at Applied Acoustics and especially Börje Wijk for all the help with the computers.

Contents

1.Introduction

1.1. Background

There has always been an interest in knowing how well a sound is transmitted through a structure. Preferably, even before it is constructed. Calculation models have been developed through the years, based on structural mechanics but they are hard to apply on a complex structure such as a multilayer wall with studs, etcetera. Nowadays, when computer processors can perform billions of calculations per second, a more detailed investigation of the sound transmission through a structure can be performed in a reasonable period of time.

1.2. Aim

The aim of this report has been to investigate the possibility to construct a computer model for calculating the reduction index of a structure. Further; to try to evaluate the quality of the computed results with other calculation models. Also trying to understand what causes the eventual differences and, finally to perform a parameter study of the material properties and geometry of the structure.

1.3. Limitations

Most of the limitations are based in the computational time, such as the resolution of the result and the investigated frequency region. But, one limitation that can not be altered by faster computers is the fact that the structure has to be flat on the side where the sound hits. The reason is that only incident angles between zero and ninety degrees are investigated in the model. Finally, the program used for the calculation has the limitation that the structure has to be finite but, this would not be a problem when doing calculations on real structures.

The structure is modeled in 2D since the calculations should cover a large frequency span (up to 5000 Hertz). If 3D would be used, the calculation time had been too long if the same frequency span would be investigated. Why a so large span is of interest is because frequencies up to 5000 Hertz is important when dealing with building acoustics.

No effort was laid on measurements due to that the results were compared with earlier calculations and those had been verified with measurements. It is of course always good to verify your results with some measurements but the modeling was the focus of this work which left no time to conduct any measurements.

1.4. Method

First, a literature study was performed in order to investigate what had been done previously on the matter of finding a reduction index of a structure and, also which properties that influences the value of the reduction index. From this knowledge collected from previous investigations, an aim of this work was set up with the help from the supervisor, Krister Larsson and the examiner, Wolfgang Kropp.

The possibility to use a finite element method (FEM) was investigated and the conclusion was that it would be possible. Therefore, the program FEMLab® was chosen due to it's availability at the Division of Applied Acoustics. The program was used to calculate the vibrations of the structure, due to a sound pressure load acting on it. Even coupled structures (both structural vibrations and air pressure differences in possible cavities) could be investigated. The results from the FEM-calculation were brought into MatLab®, where the final calculations were performed in order to end up with a reduction index.

When the model worked satisfactory; a parameter study was performed where the material properties of the structure was changed in a controlled manner. Conclusions of the results from the parameter study was drawn, both to get a confirmation of the model and the influence material properties have on the reduction index.

2.Literature survey

The transmission of audible sound through building partitions has been under study for almost one hundred years now. One of the pioneers was R. Berger, according to [4], who found a model for calculating the transmission coefficient. It was based on a single leaf wall with zero bending stiffness. Of course this was a far from complete model but it was an early mass-law model.

The aim for most of the scientists were/is to understand what influences the transmission through a building partition, e.g. a wall. With better knowledge of the subject one could understand that the double leaf wall is superior to the single leaf wall when it comes to reducing the sound passing through it. This is true for light constructions which are popular today due to constructional and economical reasons.

Cramer [2] made a model of two parallel plates with an air gap between which is a so-called double leaf wall. His model considered a soft and a stiff plate where the critical frequency of the stiff plate is assumed to lie below the frequency region of interest. The reason for this was so its radiation efficiency may be taken as unity for all practical purposes, no matter if the plate is excited structurally or by air borne sound. In reality this works well for e.g. a heavy brick wall covered with plaster board panels.

Fahy [3] also developed a model for double leaf partitions. This model does not have a restriction on one of the plates as Cramer had. It is modeled as two plates mounted on springs and dampers with properties as of the medium (e.g. air) in between. With this model he found out that at the mass-air-mass resonance frequency, the maximum of the transmission coefficient occurs. Below this frequency the double wall can be estimated as a single wall with a total mass equal to the sum of the two plates. Consequently, the mass-law is valid. (See chapter 3.) In order to minimize transmission at resonance, the plates can be chosen to have unequal mass per unit area but, the drawback is that the performance at higher frequencies is reduced.

The models described have not considered the coupling between the two plates and what affect this have on the transmission loss. Fahy has developed yet a model where he takes advantage of some earlier results relating to scattering of waves in plates by discontinuities and to sound radiation by line forces. Why line forces are considered is because the model is based on a timber stud partition. Further, the studs are assumed dynamically independent of each other (reasonable on a

frequency-average basis) and as rigid. These assumptions restrict the attenuation to bending waves incident normally on the stud-leaf connection. Except near the mass-air-mass frequency, the minima in sound reduction index are associated with resonances of the cavity. Hence the ratio of stud-transmitted power to air-transmitted power, in the frequency range of cavity resonances, is approximately unity when choosing values typical for double-leaf constructions. This means that the sound reduction index is not likely to exceed that given by the mass law for the total mass of the partition. Measurements also confirm this, which should not be too surprising since both the acoustic resonances and the studs force the two panels to vibrate with similar velocities.

A more resent study was performed by Brick [1]. She investigated the vibration and radiation of two plates, which are discontinuously coupled and compares it to the continuously coupled case. One of the plates is excited by a point source and the other is the interesting one, in a radiation point-of-view. Further, she adjusts the stiffness of the plates individually, hence trying to affect the influence of the discontinuous coupling. The model agrees quite well with her measurements. From the results she draws the conclusion that the radiation efficiency of structures of equally stiff plates can not be decreased by discontinuous coupling; whereas, a structure of unequally stiff plates can lead to a reduced radiation efficiency. The non uniform transmission of the vibration of the stiffer plate to the softer influences the vibration pattern of the softer plate. It supports the appearance of a mode shape, whose wavelength corresponds to the periodicity of the stiffness pattern of the coupling. This is the reason for the reduced radiation efficiency.

In reality when a double wall is constructed, the plates (e.g. gypsum boards) have to be fastened somehow to the framework (e.g. wooden studs). An investigation [5] was made in order to see if the spacing of the connectors (in these case screws) has anything to do with the sound reduction index of the wall. The results show that screw spacing had a great effect in double walls where each gypsum board layer was attached to each side of a timber frame. If the screw spacing is less than one half bending wavelength of waves on the gypsum board, they behave as a continuous line and if more than one half wavelength as a discrete point. In addition, when the connection between the gypsum board and the frame behaves as points then the structural coupling is proportional to the number of nails and increasing the number of screws will increase structural transmission. In the case of a double wall where the framework is divided up into two parts, one for each plate with an air gap in between, the spacing of the screws does not have any noticeable influence on the transmission. The reason is that there is no structural transmission.

All the research that has been made has contributed to the development of various standards in building acoustics. For example, there exists standards where it is strictly stated how to measure the reduction index of a building partition, both air-borne and structure-borne sound, in order to get uniform results. Why this is necessary is because some standards also contain requirement on the index, i.e. minimum levels.

The calculation models found in literature makes a good approximation of the reduction index but if you want a more detailed result there is not much to find. Most of the times measurements are the best way to get the desired information but they are expensive and time consuming. Therefore, an investigation of a possible finite element model for this purpose is presented in this paper.

3.Theory & Background

3.1. Reduction index

The reduction index is a function of frequency and measures how much the sound is reduced when passing through a structure, for example a wall. It is the difference between the incident power and the transmitted power.

$$\tau = \frac{W_{in}}{W_{trans}} \qquad \tau \text{ is the } \textit{transmission coefficient} \qquad (3.1)$$

$$R = 10\log\left(\frac{1}{\tau}\right) \qquad R \text{ is the } \textit{reduction index} \qquad (3.2)$$

The power which is not transmitted is reflected or absorbed in the structure and transformed into heat. The amount of power which is not transmitted (reduced) is different for different frequencies of the sound. There are some specific frequencies where the reduction is bad and the reason for this will be explained in this chapter.

3.1.1. Single wall

For a wall consisting of an isotropic plate of a homogeneous material, the reduction index follows the so-called *mass-law* at lower frequencies. This means that the reduction index is mass controlled and that a doubling of the mass per unit area or a doubling in frequency (one octave higher) will increase the reduction index by 6 dB. (I.e. the transmitted power is decreased by a factor four.) Since the waves in the plate are dispersive, their wavelength is not changing linearly with frequency as the case is for air. This means that there is a specific frequency where the wavelengths in air and in the structure are exactly the same and, this frequency is called the *coincidence frequency.* That is one of the frequencies for which the transmission is good because the plate and the air interact with each other and, they do not hinder each others movement when the waves are propagating with the same wavelength and speed. The exact value of the coincidence frequency depends on the angle of incidence of the incoming wave, why there can be many coincidence frequencies for a plate. Coincidence can only occur above the so-called *critical frequency*, f_c. Above the critical frequency the transmission is stiffness controlled, leading to a greater increase per octave of the reduction index than when it is mass controlled. [3]

3.1.2. Double wall

For a theoretical double wall, consisting of two isotropic plates of a homogeneous material coupled together only by an air gap, there are two more specific frequencies of interest. The one which appears lowest in frequency is the *double wall resonance*, f_0. Below this frequency the wall behaves as if it would consist of only one plate, following the earlier described mass-law. (The plates move in phase.) The air in between the plates can be seen as a spring connected to the two plates. The spring constant depends on the properties of the air (molecular density, etc.) and is therefore changing if the temperature and/or pressure vary. Further, if the space is filled with another kind of gas, the "spring" will have different characteristics.

A spring connecting two masses has a resonance frequency where the masses move in anti phase to each other. At this frequency, very little force is needed to move the mass and, the movement of one mass will easily be transmitted to the other. Hence, at this resonance a double wall will transmit a large portion of the incoming power, leading to a very low reduction index.

Above the double wall resonance the plates can move independently of each other, leading to an increase of the reduction index by 18 dB per frequency doubling (octave). This fast increase of the reduction index is stopped when the influence of the cavity resonances appears. At these frequencies (above f_d) the reduction index has an increase of 12 dB per octave until the earlier explained critical frequency is reached. Depending on the geometry of the double wall, the cavity resonances can appear higher in frequency than the critical frequency but, for the most commonly used wall geometries this is not the case.

As a conclusion of the specific frequencies mentioned; the amplitude of the reduction index around them depends on damping. For f_0 and f_d, it is the damping in the air (gas) between the plates that controls the reduction index and, the amplitude around f_c depends on the damping coefficient (η) of the material in the plates.

3.2. Hand calculation of the reduction index

A method for calculating the reduction index of a double wall will be presented and also it's restrictions. The method is assuming two infinite parallel plates with only air in between. The damping in the air is unknown which makes the value of the reduction index at the double wall resonance unknown as well. Further, the cavity resonances do not show up as dips in the reduction index. Still their influence can easily be seen when using this method.

Figure 3.1: *The sound hits the wall at plate 1, travels through the air and then leaves at plate 2.*

Starting with the low frequencies below the double wall resonance (f_0), the reduction index follows the mass-law.

$$R = R_{mass\,law} = 20\log(2m) + 20\log(f) - 49 \text{ [dB], for } f < f_o \tag{3.3}$$

m is the mass per unit area of one plate, thus $2m$ is the total mass per unit area of the wall. (The air is seen as mass-less.) The factor 49 dB comes from integrating the power over all incident angles (diffuse sound field). This factor is changed to 47 dB when dealing with finite plates because; the integration does not have to include all angles in this case. (Angles close to grazing incidence do not contribute much to the input power of a bounded plate [3].)

Since it is assumed to be only air in the gap and, further; that the plates have the same mass per unit area, the double wall resonance can be approximated by:

$$f_0 = \frac{85}{\sqrt{md}} \text{ [Hz] ,where } d \text{ is the distance between the plates.} \tag{3.4a}$$

The approximation comes from the resonance of a mass-spring-mass system. The derivation follows this procedure: (ω is the angular frequency and k the spring constant.)

$$\begin{aligned}
&\omega_{res}^2 = k\left(\frac{1}{m_{plate1}} + \frac{1}{m_{plate2}}\right) = \left\{m_{plate1} = m_{plate2} = m\right\} = \frac{2k}{m} \Rightarrow \\
&\Rightarrow \omega_{res} = \sqrt{\frac{2k}{m}} \Rightarrow \begin{Bmatrix} \omega_{res} = 2\pi f_{res} \\ k = \frac{\rho_{air} c_{air}^2}{d} \end{Bmatrix} \Rightarrow 2\pi f_{res} = \sqrt{\frac{2\rho_{air} c_{air}^2}{md}} \Rightarrow \\
&\Rightarrow f_{res} = \sqrt{\frac{\rho_{air} c_{air}^2}{2\pi^2 md}} \approx \sqrt{\frac{1.21 \cdot 343^2}{2 \cdot 3.14^2 md}} \approx \frac{85}{\sqrt{md}} = f_0
\end{aligned} \tag{3.4b}$$

Above f_0 the plates can move independently of each other, as mentioned earlier. This will lead to another way of calculating the reduction index. The mass-law is still present in the formula but, now the mass dependence concerns one plate at a time.

$$R = R_{mass\,law,\,plate\,1} + 20\log(fd) - 29 + R_{mass\,law,\,plate\,2} \text{ [dB], for } f_0 < f < f_d \qquad (3.5)$$

Because the plates are assumed to be identical, the reduction index can be calculated by:

$$R = 2R_{mass\,law,\,plate\,1} + 20\log(fd) - 29 = \ldots = 40\left(\log\left(m\sqrt{f^3 d}\right)\right) - 127 \qquad (3.6)$$

When f_d is reached, the cavity resonances will destroy this rapid increase of the reduction index. Therefore a change in the formula for the reduction index has to be made.

$$f_d = \frac{55}{d} \qquad (3.7)$$

$$R = R_{mass\,law,\,plate\,1} + 6 + R_{mass\,law,\,plate\,2} \text{ [dB], for } f_d < f < f_c \qquad (3.8)$$

This can, since the earlier mentioned symmetry, be simplified to:

$$R = 2R_{mass\,law,\,plate\,1} + 6 = \ldots = 40(\log(mf)) - 92 \qquad (3.9)$$

The next frequency of importance is the critical frequency, f_c. This is when the wavelength of the vibrating plate matches the wavelength of the sound wave in the surrounding air. The critical frequency is easily calculated if the material dependent coincidence number (K_c) of the plate, is known.

$$f_c = \frac{K_c}{h} \quad \text{,where } h \text{ is the thickness of the plate.} \qquad (3.10)$$

If the coincidence number is unknown, f_c can be calculated by finding the frequency where the wavelengths are the same. Since bending waves on a plate are the dominating ones when it comes to sound radiation, the formula for such wavelengths (λ_B) is used.

$$\lambda_{air} = \lambda_B \Leftrightarrow \frac{c_{air}}{f} = \frac{c_B}{f} \Rightarrow c_{air} = c_B \Rightarrow c_{air} = \sqrt[4]{\frac{B}{\rho S}\omega^2} = \left\{ \begin{matrix} B = \text{bending stiffness} \\ \rho = \text{density of plate material} \\ S = \text{area of cross section} \end{matrix} \right\} =$$

$$= \sqrt[4]{\frac{EI}{\rho S}(2\pi f)^2} = \sqrt[4]{\frac{E\frac{bh^3}{12}}{\rho bh}(2\pi f)^2} = \sqrt[4]{\frac{Eh^2 f^2 \pi^2}{3\rho}} \Rightarrow$$

$$\Rightarrow f = \frac{c_{air}^2}{h\sqrt{\frac{E\pi^2}{3\rho}}} = f_c \qquad (3.11)$$

This is exactly how the coincidence number is calculated for a plate material. It depends on the Young's modulus (E), the density (ρ) and the speed of sound in the surrounding medium.

$$K_c = \frac{c_{medium}^2}{\sqrt{\frac{E\pi^2}{3\rho}}} \text{ [m/s]} \qquad (3.12)$$

The reduction index at the critical frequency is calculated by:

$$R = 2\left(R_{masslaw,plate1} + 10\log\eta + 8\right) \text{ [dB] for } f = f_c \qquad (3.13)$$

For frequencies above f_c, the reduction index can be calculated by the following formula (identical plates):

$$R = 2\left(R'_{masslaw,plate1} + 10\log\left(\frac{f}{f_c} - 1\right) + 10\log\eta - 2 \right) + 6 \text{ [dB] for } f > f_c \qquad (3.14)$$

The $'$ in $R'_{masslaw,plate1}$ indicates that the reduction only is calculated for a single incoming plane wave at normal incidence and, η is the loss factor for the plate.

A calculation of the total reduction index, spanning from below f_o to above f_c is shown in figure 3.2 below. The data of the calculated wall is shown in table 3.1.

h	=	0.013	[m]	m	=	10.4	[kg/m^2]
ρ	=	800	[kg/m^3]				
E	=	2.0E+09	[Pa]	K_c	=	41	[m/s]
c_{air}	=	343	[m/s]				
η	=	0.02	[-]				
d	=	0.1	[m]				

Table 3.1: *The left column of the table is the material data and the values in the right column are calculated from these. The mass per unit area (**m**) is a function of thickness of the plate (**h**) and the density of the plate (**ρ**). The coincidence number (K_c) is a function of Young's modulus (**E**), speed of sound in air (c_{air}) and **ρ**.*

Since the calculations have quite sharp transitions between the different frequency regions, a smoother curve is hand sketched on the graph. Another reason for making a hand sketch is that some values are not representing reality in a good way. For example at $f > f_c$, the reduction curve should not start at 0 dB.

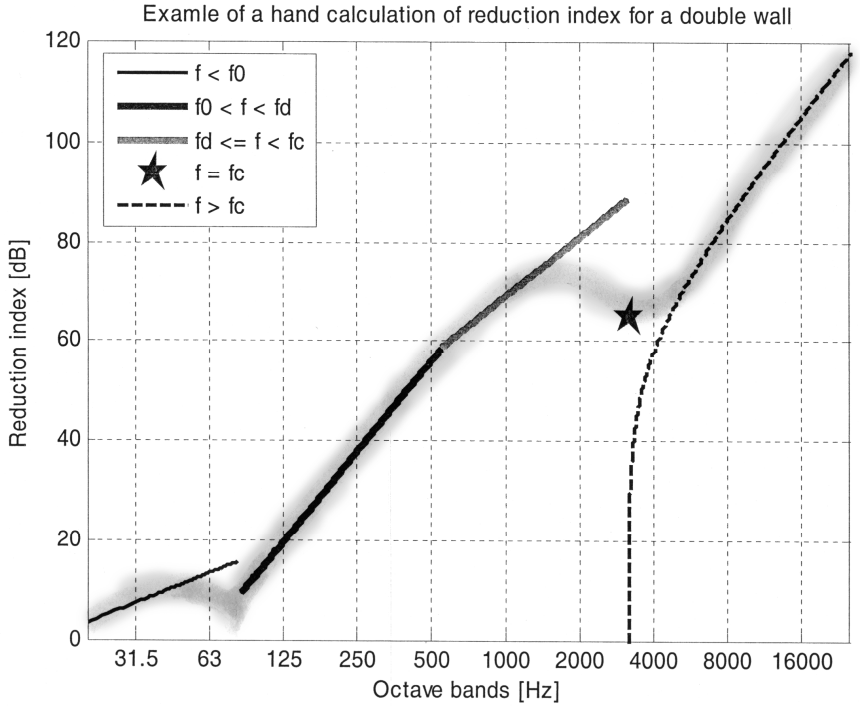

Figure 3.2: *Reduction index calculation of an arbitrary double wall. The sketched curve on top of the calculated is a better representation of reality and, the shape depends on the damping in the structure. (Note that the added curve is only an approximation.)*

3.3. ISO 717-1

When choosing the right building partitions between two rooms, it is complicated to compare a reduction curve for each possible solution. Since the human ear is constructed to be more sensitive to some frequencies and, sounds in offices and residential houses are quite well defined, it would be good to weigh the reduction curve with these known facts in order to get a single number for the sound insulation quality of a wall. That is why this standard was developed.

The ISO standard number 717 part 1 deals with how it is possible to reduce a reduction index curve into a single number, the so called *weighted reduction index*, R_w. The standard is mostly used when a reduction curve is obtained from a lab measurement or an in-situ measurement. This chapter deals with how values of a reduction index in 1/3-octave bands can be transformed into a single value R_w.

The values in 1/3-octave bands, obtained from a measurement are adapted to a reference curve which is constructed according to the properties of the human ear. The reference curve only contains values from the 100 Hertz 1/3-octave band to the 3150 Hertz band. Therefore, the weighted reduction index is not affected by changes above or below those 1/3-octave bands. The ISO-standard states that the reference curve should be shifted towards the measured curve, by steps of 1 dB, until the sum of the unfavorable deviation is as large as possible but not more than 32,0 dB. R_w is then the value of the reference curve at 500 Hertz. It is probably easier to understand by looking at figure 3.3.

What are meant by unfavorable deviations are those 1/3-octave bands where the reference curve is above the measured curve. The sum of the differences at those 1/3-octave bands should be as large as possible but not more than 32 dB. At, for example 250 Hertz, the deviation is approximately 10 dB which is a large part of the total sum. Hence, a dip like that has a quite large effect on the weighted reduction index (the triangle in the graph). For this imaginary wall, the weighted reduction index is 45 dB which is a good value for a wall separating two rooms where people speak in a normal voice (e.g. two offices).

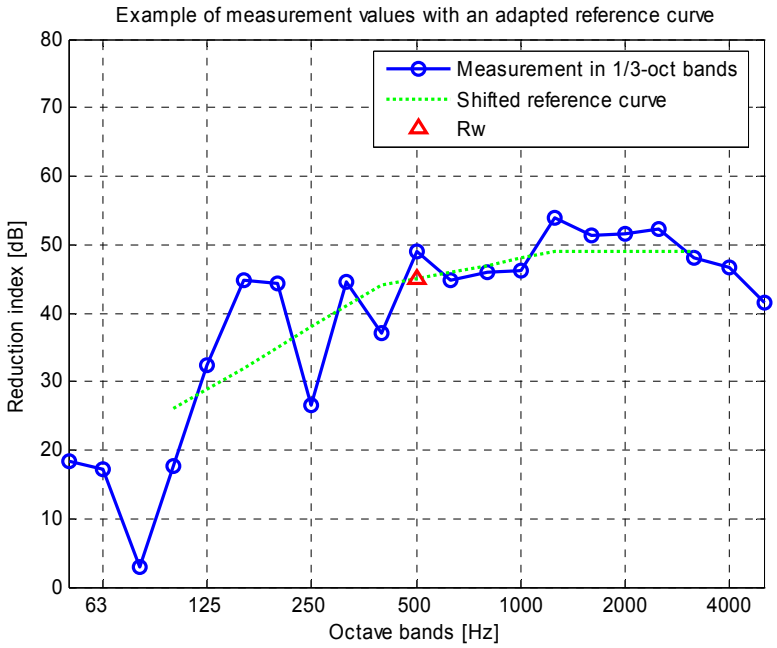

Figure 3.3: *Graphical presentation of how the weighted reduction index of a wall is found. The measurement curve is only an example of the reduction index of a double wall with studs (i.e. not only air-coupling).*

The ISO 717-1 will later be used when analyzing the results from the calculation model (chapter 4). This will give a good value of how well the tested walls in the parameter study (chapter 5) reduce the incoming sound. The model is constructed in such a way that the results could be taken from a lab measurement, why it is permissible to use the ISO-standard.

4.Modeling

4.1. Model description

4.1.1. Overall description

The goal for the model is to give a good approximation for the sound reduction index of an arbitrary structure, separating two gas volumes. In order to do this, one has to know the amount of energy that is transmitted in to the structure due to the sound pressure acting on it. When this is known for the entire contact surface, it is possible to calculate the vibration pattern of the entire structure. Therefore, it is also possible to calculate the velocity of the part of the structure which is in contact with the opposite gas volume. The pressure can thus be calculated by the Rayleigh integral and further also the output energy. The reduction index can easily be computed when knowing the input and output energy.

4.1.2. Assumptions and restrictions

The normal projection of the sound wave, which hits the object in normal direction to the surface, is assumed to reflect all of its energy out from the structure. This assumption can be made for relatively hard walls with a reduction index of more than approximately 20 dB.

The model takes advantage of the fact that studs that connect two plates usually are very long, in comparison to its height and width. Hence the model is reduced to 2D which decreases the calculation time enormously.

Finally, there is no load on the structure from the air on the opposite side (the radiating side). This gives an impedance of zero on the radiating boundary. The sound radiation was calculated separately in the post-processing and was not included in the FEM calculations.

4.1.3. Finite Element modulation

The structural vibrations due to the sound pressure load are calculated with the Finite Element Method (FEM), using the program FEMLab®. A *Plain Strain* 2D

model is used, which means that a cross section of the structure is investigated with the assumption that there is no deformation along the z-direction (the third dimension). For the air part in the model (when the structure contains cavities) the 2D Helmholtz's equation is used. The 2D limitation give that the wave number is equal to zero in the z-direction.

The load distribution on the structure depends both on incident angle and frequency of the sound wave. Therefore, a number of calculations are made, one for each angle containing the vibration behavior at all chosen frequencies. Why more than one incident angle has to be considered is because the reduction index is assuming diffuse sound field acting on the structure. Further, in theory, an incident angle has one specific frequency where there is total transmission, which is also an argument to consider more than one angle.

In order to get the influence from the structural vibrations and air pressure differences, a coupled model had to be created (if the structure contains some sort of air volumes which is the case for a double wall). What is meant by coupled is that the vibration of a plate has to create pressure difference in the air on their common boundary. Therefore, a change in air pressure has to create a load on the plate. If the displacement of the plate (the boundary) is known, the normal acceleration can by calculated with the help of the excitation frequency as follows:

Displacement = x (4.1a)

Velocity = $j\omega x$ (in the complex plane) (4.1b)

Acceleration = $-\omega^2 x$ (in the complex plane) (4.1c)

where $\omega = 2\pi f$ and f is the excitation frequency

The acceleration of the boundary in normal direction (***n***) is directly proportional to the air pressure on the same boundary. The change in sound pressure due to the acceleration can be calculated as: (Compare with Newton's second law; $F = m\,a$)

$$\frac{\partial p}{\partial \boldsymbol{n}} = -\rho \frac{\partial v_n}{\partial t} = -j\omega\rho v_n = -\rho a_n \qquad (4.2)$$

,where ρ is the density of the adjacent material. ($p \propto a$)

It is important to know if the normal direction is in positive or negative direction according to the coordinate system used in the model, in order to know if the acceleration is increasing or decreasing the pressure. Accordingly, the direction of the load on the plate from the air pressure is equally important.

The mesh resolution of the model is determined by the bending wavelength of the plate. In order to get good enough results, the mesh elements (i.e. the longest side of a triangle in the triangulated mesh) have to be as small as the length of one sixths of the bending wavelength. The bending wavelength is calculated as follows:

$$\lambda_B = \frac{c_B}{f} \quad \text{,where} \quad c_B = \sqrt[4]{\frac{B}{\rho S}\omega^2} \tag{4.3}$$

Since the model also could contain air, the wavelength in air has also to be considered when choosing an appropriate mesh. The shortest wavelength at the maximum frequency of interest is dominating the choice of mesh resolution. At high frequencies, the wavelength in air is shorter than on the plate and at low frequencies it is the other way around. The break point is the critical frequency of the plate. (See chapter 3 for details about the critical frequency.)

The elements used in the model are of the type *Lagrange – Quadratic* which means that the solutions at the nodes in the mesh are not connected by linear function but by a polynom of second order. This gives a smaller error of the solution than if *Lagrange – Linear* elements would be used.

When the correct mesh is chosen, the pressure distribution on the structure has to be set. The pressure acts as a negative or positive load on the plate, causing it to move up or down. Since plane waves are considered, only the perpendicular transpose of each wave contributes to the input load.

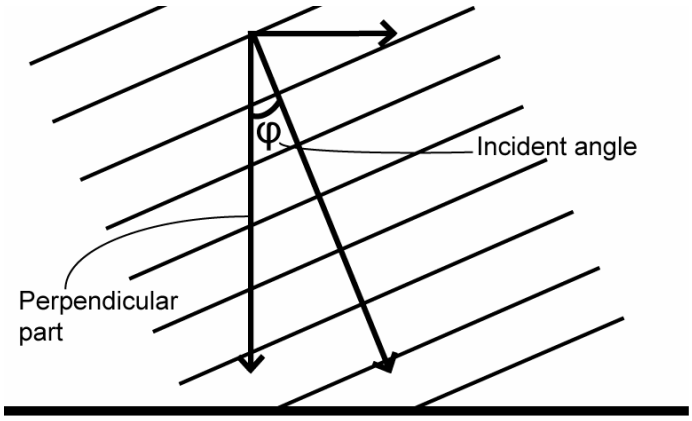

Figure 4.1: *Division of the incoming plane wave into normal (perpendicular) and tangential part.*

This will lead to that an incoming wave with an incident angle equal to 90 degrees (gracing incidence), does not give any energy transmission (in the finite element model) even though there is a pressure distribution.

The load acting on the structure is both dependent on incident angle and frequency of the approaching plane wave. The frequency dependence comes from the wave number *k*, which is equal to $2\pi f/c$ where *c* is the speed of sound in air.

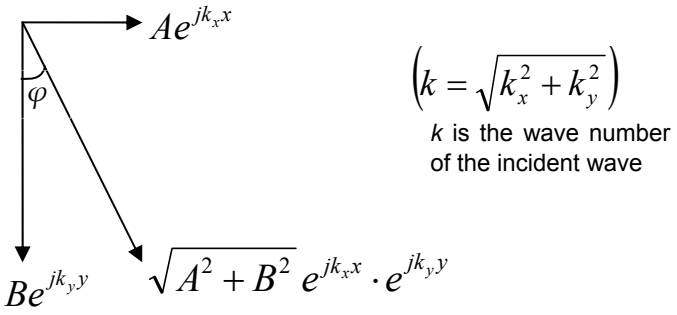

Figure 4.2: *The perpendicular part of the incoming wave contributes to the input power in the structure.*

Because of the assumption that all the energy is reflected on the surface of the structure, the total pressure on the surface is two times the pressure of the incident wave. This gives the load:

$$F_y = -2e^{jk\cos(\varphi)x} \quad \text{,where } _y \text{ indicates a load parallel to the y-axis.} \qquad (4.4)$$

The minus sign is due to the way the coordinate system is set in the model and, the *x* in equation (4.4) is also linked to the coordinate system. (See fig. 4.3.) The load is changing over the x-direction.

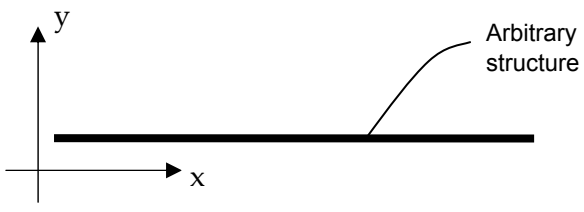

Figure 4.3: *Definition of the coordinate system in the model.*

Finally the boundaries at the end of the plates have to be defined and, a rigid connection is chosen in order to mimic a real structure (wall) as good as possible.

The choice of boundary conditions has most influence on the reduction index at low frequencies since that is when the influence wave has longest wavelength. A closer investigation of how long the structure has to be in order to get reasonable values for the reduction index, shows that at least a 3 meter wide structure (wall) has to be used. Of course an even wider structure will give better results in the low frequency region but, it is a matter of calculation time. (Some calculations were made with a 10 meter wall for better detail. For example figures 4.6 and 4.7.)

4.1.4. Post processing

What is called the post processing is the calculation of the reduction index from the obtained velocities from the FE-calculation. The velocities of interest are only those of the radiating plate because, the velocity of the boundary where the sound wave (plane wave) hits can easily be calculated as:

$$v = \frac{e^{jk\cos(\varphi)}}{\rho c}\sin(\varphi) = \frac{p}{\rho c}\sin(\varphi) \tag{4.5}$$

The input energy is calculated using the following formula:

$$W_{in} = \frac{1}{2}\mathrm{Re}\left[p \cdot q^{*}\right] \text{ ,where } q \text{ is the flow velocity. } \left(q = v \cdot meshsize\right) \tag{4.6}$$

The output energy can be calculated from the velocity of the radiating plate via the pressure it creates in the far field. Why the pressure is calculated in the far field instead of directly on the plate, is to avoid singularities when using the Rayleigh integral. (If the pressure is calculated in one point, from to the velocity in the same point, one will end up with a zero in the denominator.) Another benefit of being in the far field is that the Hankel function in the Rayleigh integral (in 2D) can be approximated by:

$$H_0^{(2)}(k,r) = \frac{j\sqrt{2\pi}}{\pi\sqrt{kr}}e^{-j(kr+\pi/4)} \tag{4.7}$$

,where $k = \frac{2\pi f}{c_{air}}$ and r is the distance from the velocity source to where the pressure is calculated.

The Rayleigh integral without this approximation is:

$$p(k,r) = \frac{1}{2}\rho_{air} c_{air} k \int_0^l v(x) H_0^{(2)}(k,r) dx \tag{4.8}$$

,where l is the length of the radiating plate in an infinite baffle.

The approximation speeds up the calculations of the total pressure tremendously (instead of using the **`besselh`** function in Matlab). The output energy can now be calculated by:

$$\begin{aligned} W_{out} &= \int_0^L \frac{1}{2}\mathrm{Re}\{p \cdot q^*\} d\xi = \int_0^L \frac{1}{2}\mathrm{Re}\left\{\frac{|p|^2}{\rho_{air} c_{air}}\right\} d\xi = \int_0^L \frac{\frac{1}{2}|p|^2}{\rho_{air} c_{air}} d\xi = \\ &= \{Discreet\ problem\} = \sum_{m=1}^{M} \frac{\frac{1}{2}|p_m|^2}{\rho_{air} c_{air}} \Delta\xi \end{aligned} \tag{4.9}$$

,where L is the length of the half sphere. (See fig. 4.4)

The calculations are made on a half sphere around the radiating plate and the M pressures from the Rayleigh integral are equally spaced on the sphere with a distance $\Delta\xi$ from each other.

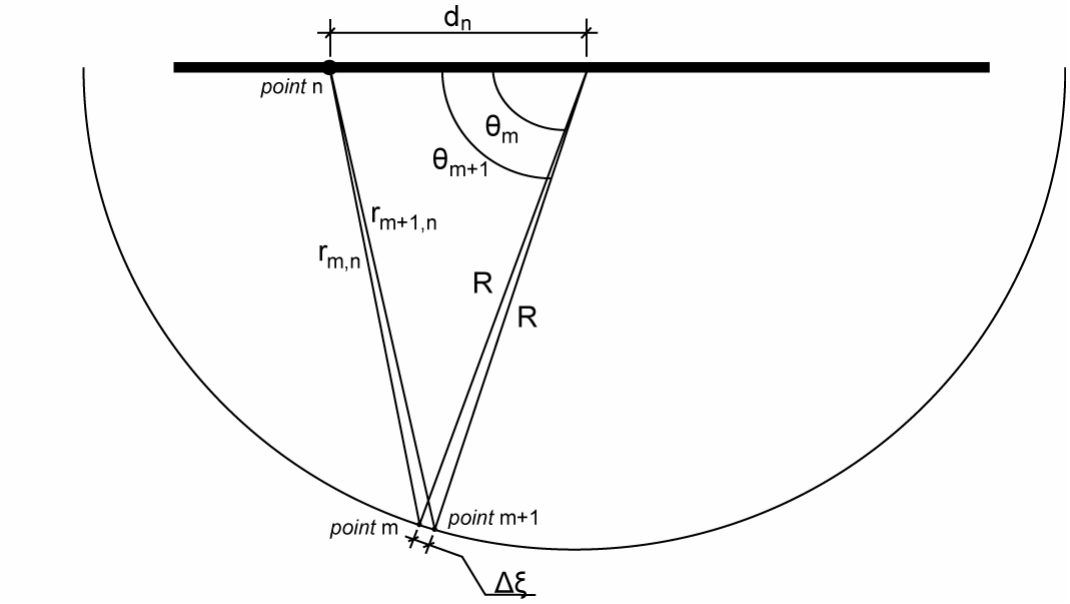

Figure 4.4: *Schematic of the pressure calculation (Rayleigh integral) from the velocities of the discreet points on the radiating plate of the wall. Length of the half sphere, L=MΔξ.*

$$\Delta\xi = \Delta\theta\, R = \left(\theta_{m+1} - \theta_m\right)R \qquad \textit{(}\Delta\xi \textit{ is small in comparison with wavelength)} \qquad (4.10)$$

$$r_{m,n} = \sqrt{R^2 + d_n^2 - 2Rd\cos\theta_m} \qquad \textit{(The cosine law)} \qquad (4.11)$$

Now when both input and output energy is calculated, the reduction index, R can be obtained via the transmission loss, τ as follows:

$$R = 10\log\left(\frac{1}{\tau}\right) \quad \text{,where} \quad \tau = \frac{W_{in}}{W_{out}} \qquad (4.12)$$

In order to know how many (equally spaced) incident angles that have to be taken into consideration, a test calculation for different number of angles was performed. The resulting reduction indices at 1000 Hertz of an arbitrary structure is shown in the graph below.

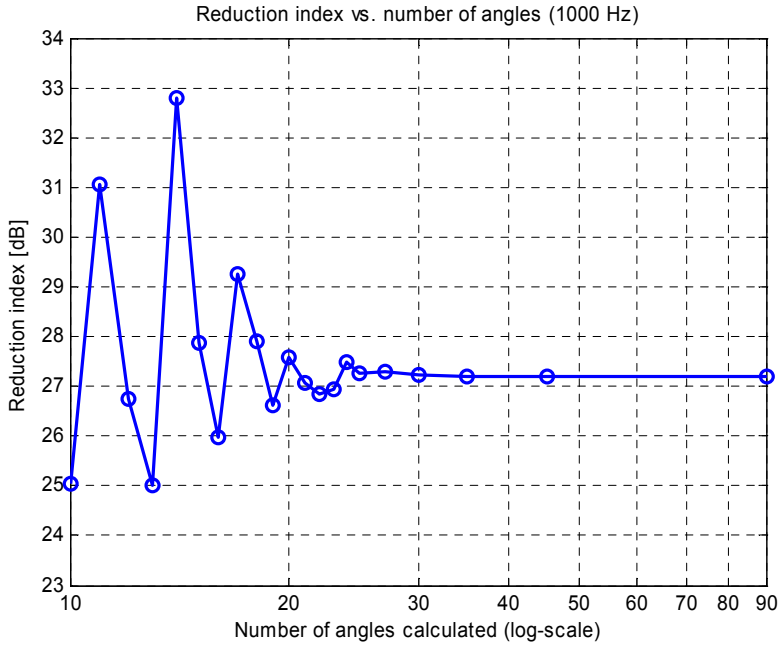

Figure 4.5: *Resulting reduction index when changing the number of incident angles calculated. Calculated on an arbitrary structure.*

The conclusion that 30 angles would give a good enough result was drawn. Because the check was made at 1000 Hertz, frequencies above that could give a slightly incorrect result for the reduction index. An increase in number of angles would of course also increase the calculation time and, to be able to manage a parameter study this angle trade off had to be made. The graph below shows how small the difference in reduction index (for a double wall) is due to the change in number of incident angles considered.

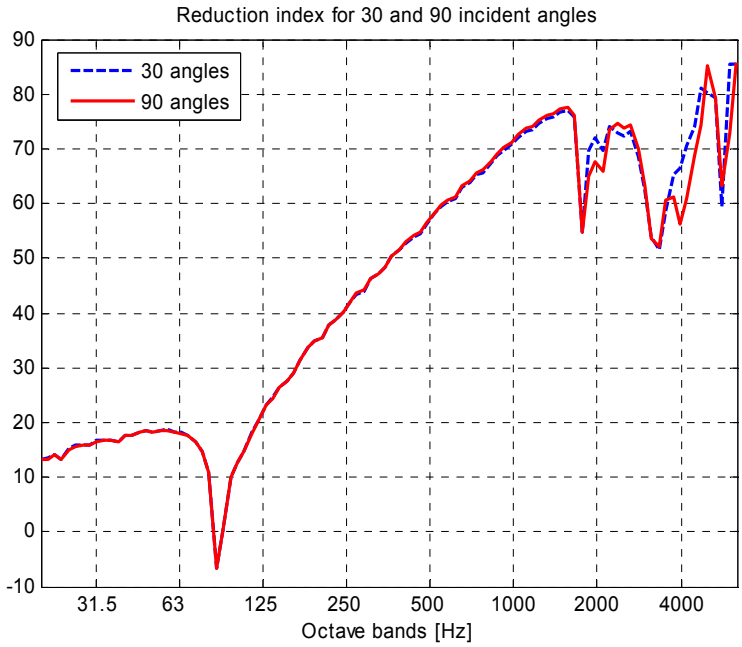

Figure 4.6: *A comparison between two reduction index calculations. One with 30 equally spaced incident angles and one with 90 angles between 0 and 90 degrees. Calculations made between 20 and 6000 Hertz of a 10 meter model of a double wall with only air coupling.*

The calculation for 90 angles naturally takes three times longer time than the 30 angles calculation.

4.2. Verification with results from literature

The theoretical method explained in chapter 3, for calculating the reduction index of a double wall, is here compared with the results from the constructed calculation model (FEM-calculation).

h	=	0.013	[m]	m	=	10.4	[kg/m^2]
ρ	=	800	[kg/m^3]				
E	=	2.0E+09	[Pa]	K_c	=	41	[m/s]
c_{air}	=	343	[m/s]				
η	=	0.02	[-]				
d	=	0.1	[m]				

Table 4.1: *Material properties of the calculated wall. Exactly the same values are used in the hand calculation as in the FEM-calculation. (Compare with table 3.1)*

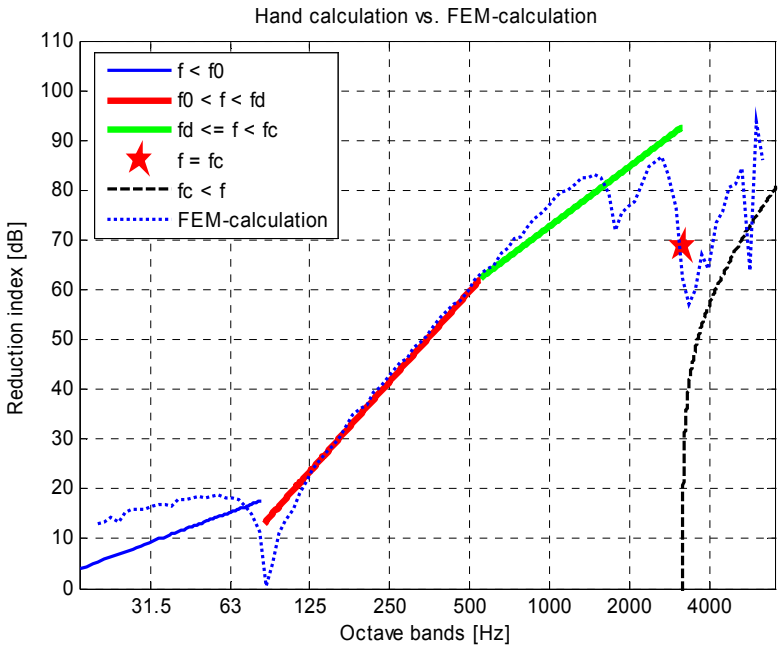

Figure 4.7: *Results from both the hand calculation and the FEM-calculation. Since the wall consists of finite plates, the factor -49 dB in the mass-law is changed to 47 dB. (See chapter 3) The FEM-calculation includes 1 percent damping in the air between the plates.*

The results from the FEM-calculation correspond well with the hand calculations. Note that these calculations only are valid for a wall that has no studs what so ever. The only coupling between the plates is air. Naturally, the FEM-calculation was performed in a similar way. There is a dip in the FEM-calculations which corresponds to the coincidence (f_c) between the plate and the air. The dip just below the coincidence is exactly where one half wavelengths fit between the plates (the first resonance between the plates). The influence from this resonance can be seen for frequencies above f_d. (See the brake point, just above 500 Hertz, of the hand calculated curve in the graph.) The influence from the first cavity resonance in the FEM-calculation appears higher up in frequency than for the hand calculation. If more damping would be added in the model, the reduction index would be influenced over a broader frequency range at the cavity resonance and, the dip would not be as strong. To fix the differences above f_d between the two calculation methods, it is not only to ad more damping in the FEM-calculation. Increased damping would give a more similar curve shape but the reduction index for the FEM-calculation would have higher overall level. (See for example fig 5.10.)

5.Parameter study

When the model was assumed to be working properly, a parameter study was performed in order to understand the influence of material properties on the reduction index. Also a study of the physical connections of the plates was made. Finally, the results were compared with the results Haike [1] obtained in her work.

5.1. Influence of parameters

The parameters that were changed were the following:

		1	*2*	*3*	*4*	*5*
1	E-mod of studs	1e7	1e8	1e9	**1e10**	1e11
2	E-mod of plates	1e7	1e8	**1e9**	1e10	1e11
3	Varying E-mod (plate 1)	1e7	1e8	**1e9**	1e10	1e11
4	Varying E-mod (plate 2)	1e7	1e8	**1e9**	1e10	1e11
5	Density of plates	200	400	**800**	1600	3200
6	Stud width (cm)	1	2	**4**	8	16
7	Stud distance (cm)	10	20	40	**60**	80
8	Damping in air	**0**	1e-5	1e-4	1e-3	1e-2

Table 5.1: *Parameters that were changed in the study. Values in bold type are default.*

The values in bold type are the ones that are held constant when one parameter is changed. These values are later referred to as default values or the default wall.

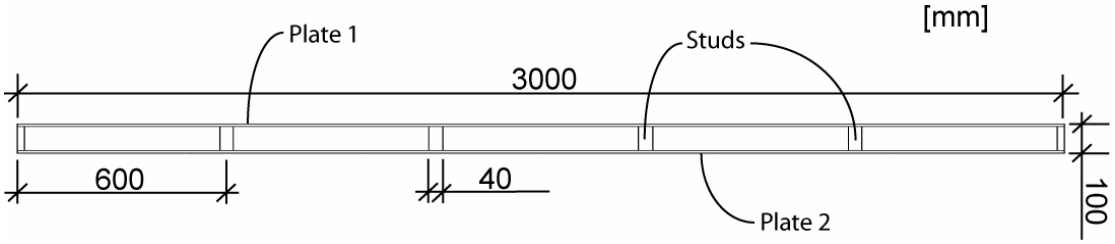

Figure 5.1: *Geometry of the default wall with definition of plates and studs. The density of the studs is held constant at 500 kg/m³. Also the damping in the plates and studs are constant at 2 percent.*

One hundred, logarithmically spaced frequencies between 20 and 6000 Hertz were calculated for each parameter setup. The results were then summed up into 1/3-

octave bands in order to more easily take in the overall picture and also to be able to calculate a weighted reduction index. The one hundred frequencies gives approximately four frequencies per 1/3 octave band which could seem a bit on the low side but, it is a matter of calculation time. (Each parameter setup takes approximately 1 hour and 15 minutes to calculate on a DualG4 Mac.) The weighted reduction index (R_w) is calculated according to the ISO 717-1 standard. It gives a single value for the reduction index which is even easier to compare for different parameter setups. The result of the parameter study in weighted reduction indices can be seen in table 5.2.

		1	*2*	*3*	*4*	*5*
1	E-mod of studs	40	42	45	**43**	42
2	E-mod of plates	46	44	**43**	32	29
3	Varying E-mod (plate 1)	47	45	**43**	40	38
4	Varying E-mod (plate 2)	48	47	**43**	41	38
5	Density of plates	24	31	**43**	54	61
6	Stud width (cm)	46	43	**43**	38	43
7	Stud distance (cm)	44	39	37	**43**	46
8	Damping in air	**43**	42	42	42	42

Table 5.2: *Results, in weighted reduction index, from the parameter study. The values in bold type correspond to the default wall, why they all have the same value. The number above and to the left of the table are the same as in table 5.1, making then easier to compare. (For example the result cell (7,2) corresponds to the parameter value in cell (7,2) in table 5.1)*

5.1.1. Young's modulus in plates and studs

First the change in Young's modulus (E-mod) of the plates and studs were investigated. It can be seen that the change of the plates has a greater influence on R_w than the change of the studs. Why the increase in E-mod of the plates results in a decrease of R_w is because the frequency of the double wall resonance also increases. Since the ISO-standard only considers 1/3-octave bands between 100 and 3150 Hertz, the double wall resonance for the softer plates appears below the first 1/3-octave band of interest. This will lead to that the fast increase of the reduction index above the double wall resonance is taken into account earlier in frequency. Hence, the walls with stiffer plates acts as single leaf partitions, following the mass-law, for a wider frequency span. A more detailed display of the results from the first two rows of the parameter study can be seen in the graphs below. (See figures 5.2 and 5.3) The results are in 1/3-octave bands from 20 to 5000 Hertz. (See table 5.3.)

20	25	31.5	40	50	63	80	100	125	160	200	250	…
…	315	400	500	630	800	1000	1250	1600	2000	2500	3150	4000	5000

Table 5.3: *List of the 1/3-octave bands (in Hertz) that are used in the calculation of the reduction index.*

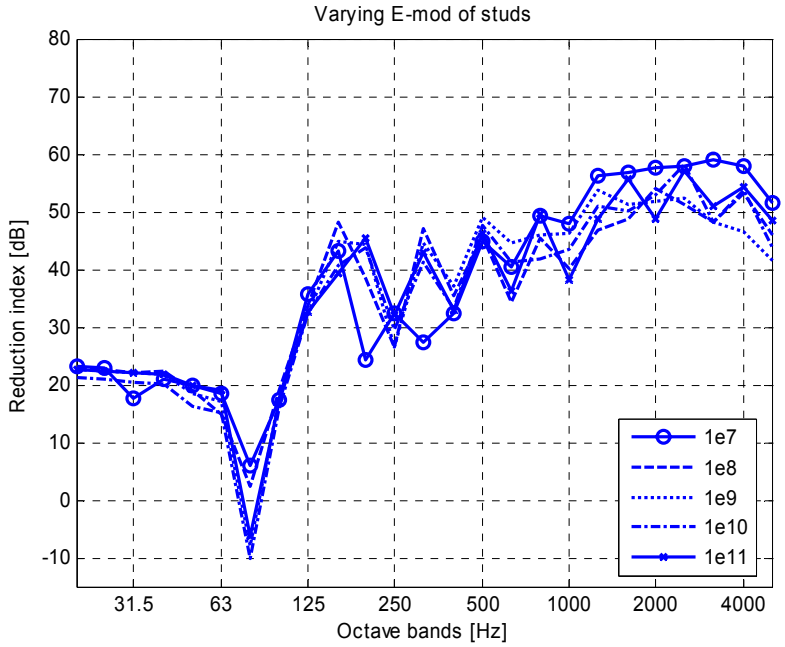

Figure 5.2: *Results from the parameter study in 1/3-octave bands between 20 and 5000 Hertz. The different curves correspond to the values of row 1 in table 5.1.*

As said earlier and which can be seen in figure 5.2, the change in E-mod of the studs does not have a large effect on the reduction index. The double wall resonance appears in the same 1/3-octave band but with different magnitudes. (Note that a reduction index below zero is in reality impossible but, since there is an assumption made in the model which only holds for a reduction index above 20 dB, a sub zero reduction index can occur, especially around the double wall resonance. See chapter 4.1.2.)

Since the model is finite, the reduction index is stiffness controlled at frequencies below the first resonance of the structure. I.e. for frequencies that have such a long wavelength that a half wavelength is longer than the model width (in this case 3 meters). For example when the Young's modulus is set to 10^{11} Pascal, the bending wavelength is so long that the first resonance of the structure is as high as 40 Hertz. (See figure 5.3.)

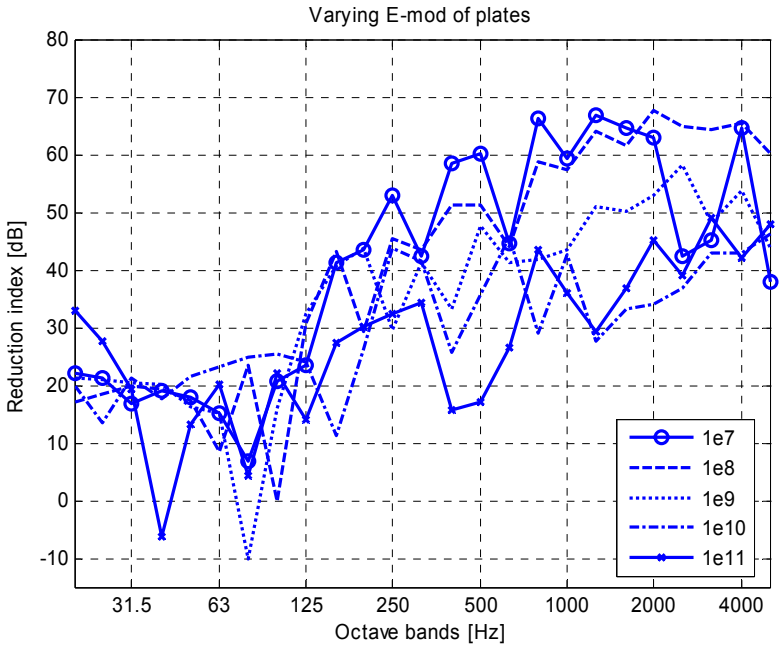

Figure 5.3: *Results from the parameter study in 1/3-octave bands between 20 and 5000 Hertz. The different curves correspond to the values of row 2 in table 5.1.*

The next parameter that was changed was the Young's modulus of one of the plates while the other was held constant (10^9 Pa). First the plate on which the sound wave hits was changed (plate 1). This gave a slightly better weighted reduction index than if both plates were changed simultaneously. A reason for this can be that it is easier to get differences in the vibration pattern of the plates, which can be seen as uncoupled plates. This is good when it comes to reducing the transmission of sound. Also here, a softer plate gives a higher R_w.

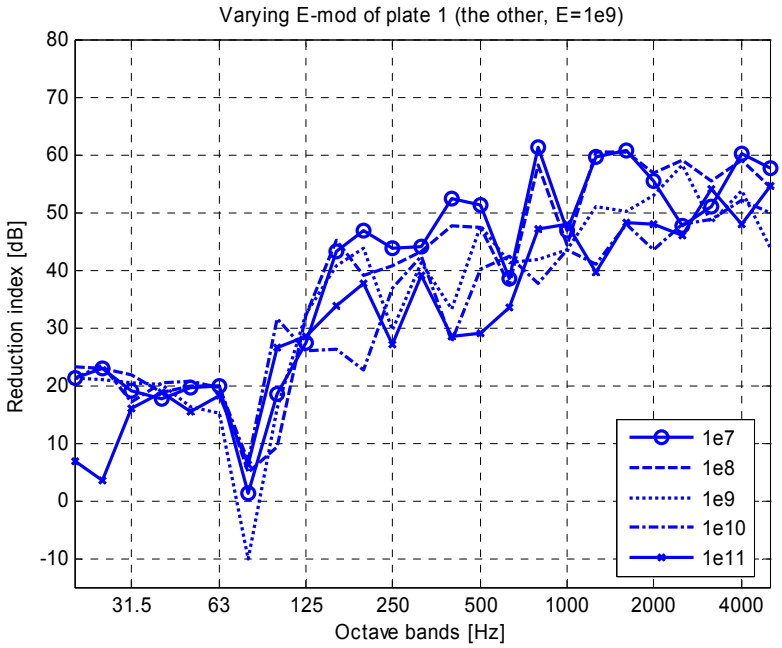

Figure 5.4: *Results from the parameter study in 1/3-octave bands between 20 and 5000 Hertz. The different curves correspond to the values of row 3 in table 5.1.*

When changing the parameter of the second plate (plate 2), an even higher value of the reduction index can be seen, especially in the high frequency region. (Compare the values of row 3 and 4 in table 5.2)

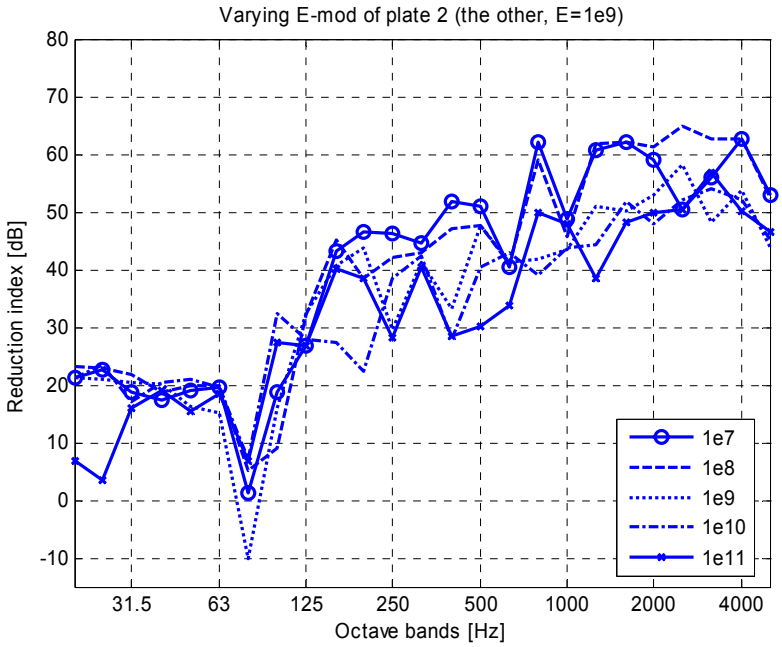

Figure 5.5: *Results from the parameter study in 1/3-octave bands between 20 and 5000 Hertz. The different curves correspond to the values of row 4 in table 5.1.*

5.1.2. Density of the plates

This parameter change is mostly done in order to see if the model behaves as would be predicted. If the density (mass) of the plates is increased, the reduction index will also increase. Figure 5.6 shows exactly that.

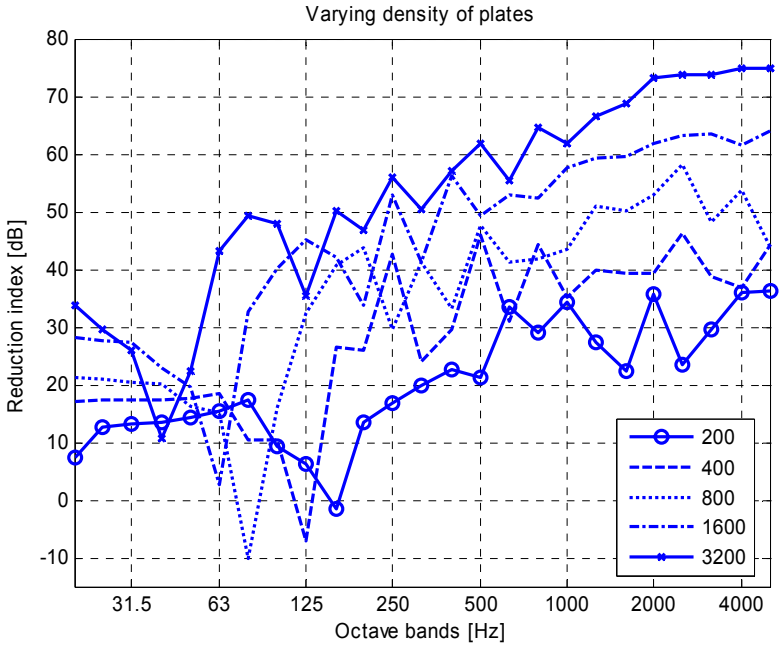

Figure 5.6: *Results from the parameter study in 1/3-octave bands between 20 and 5000 Hertz. The different curves correspond to the values of row 5 in table 5.1.*

Note that the weighted reduction index does not change linearly (See table 5.2, row 5.) when the density is increased (doubled) even if the distance between the reduction lines in the graph seem to be equally spaced in the high frequency region. Again, it depends on in which 1/3-octave band the double wall resonance appears, since R_w is only calculated from the 100 Hertz 1/3-octave band. (Look at the reduction index at 125 Hertz in figure 5.6. Those values are not equally spaced.)

5.1.3. Stud width and distance between studs

The change of stud width and distance between the studs has a quite large influence on the weighted reduction index. When looking at the graphs one has to have in mind that the total mass of the wall also will change when changing the stud width and distance. (ρ_{stud}=500 kg/m^3) This leads to, for example when the distances between the studs are only 10 centimeters; it acts more as a heavy single leaf wall than as a double leaf wall. (The double wall resonance appears above 2000 Hertz! See figure 5.8.)

Compare the values of stud width and distance between the studs with the default wall in figure 5.1, in order to get a better understanding what the changes do to the wall's geometry.

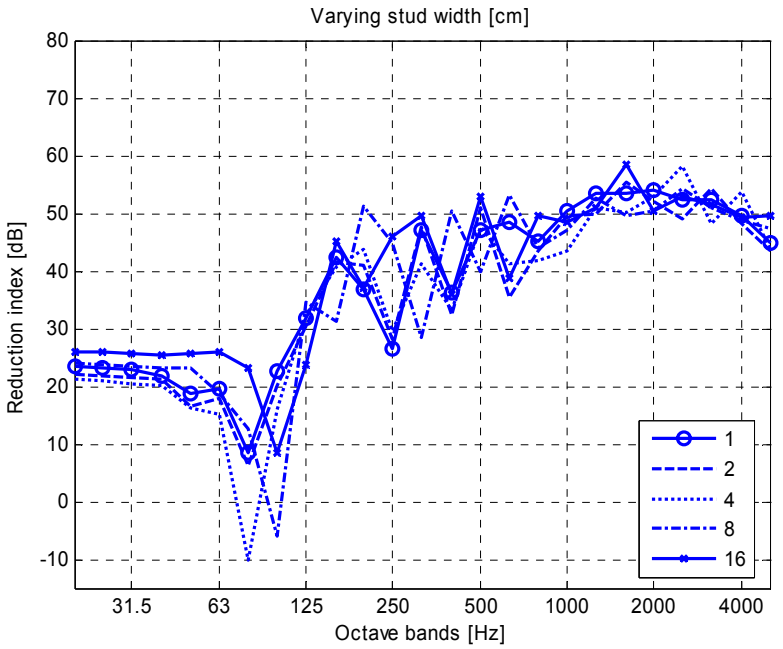

Figure 5.7: *Results from the parameter study in 1/3-octave bands between 20 and 5000 Hertz. The different curves correspond to the values of row 6 in table 5.1.*

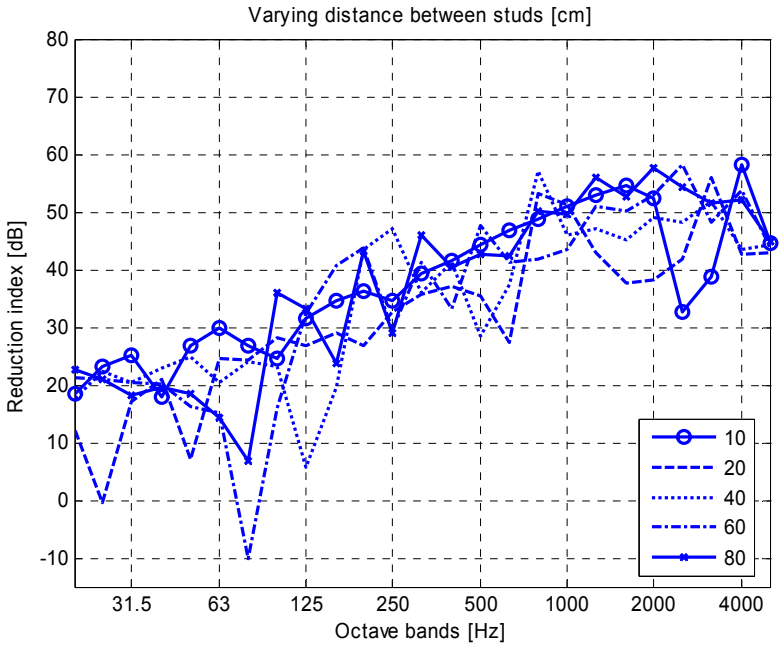

Figure 5.8: *Results from the parameter study in 1/3-octave bands between 20 and 5000 Hertz. The different curves correspond to the values of row 7 in table 5.1.*

It can be seen that when the stud widths are 8 or 16 centimeters, the double wall resonance appears in a higher 1/3-octave band than if the studs have a width of 1, 2 or 4 centimeters. (See figure 5.7) This is because when the width is changed, also the width of the free span (of the plates) between the studs is changed. Hence, the "spring" is stiffened up, leading to a higher resonance frequency.

5.1.4. Damping in the air

In the previously mentioned default wall, there is no damping in the air between the plates. If such damping is introduced in the model (by using a complex speed of sound, $c=c_0(1+i\eta)$) the results do not show the expected results at first. As can be seen in the table 5.1, the values are all the same and lower if damping is included. Figure 5.9 shows the same results.

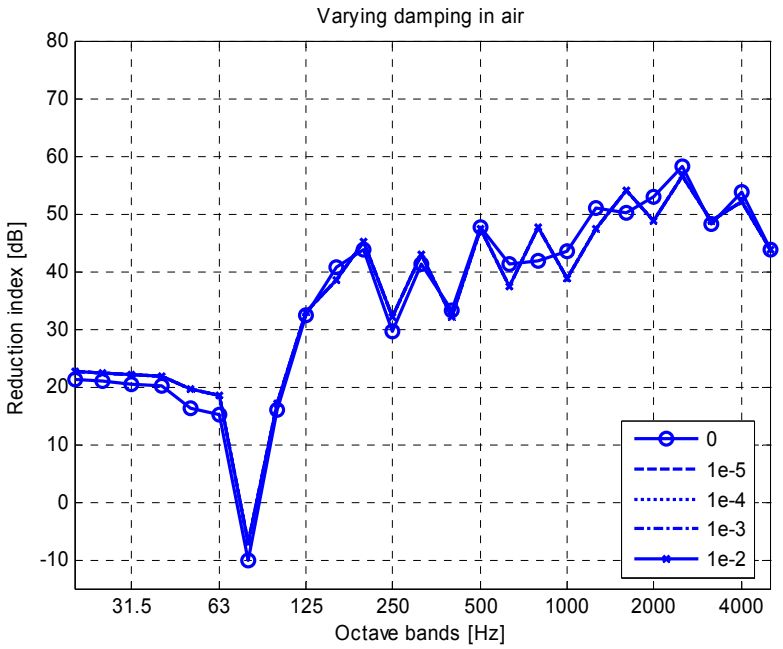

Figure 5.9: *Results from the parameter study in 1/3-octave bands between 20 and 5000 Hertz. The different curves correspond to the values of row 8 in table 5.1.*

To see if damping could be used in the model in a correct way, a more detailed calculation of a double wall with no studs was made; one calculation with no damping and two with differently strong damping in the air. Figure 5.10 shows a more satisfying result than figure 5.9. I.e. the peaks (resonances) are not as strong for the damped models as for the un-damped one.

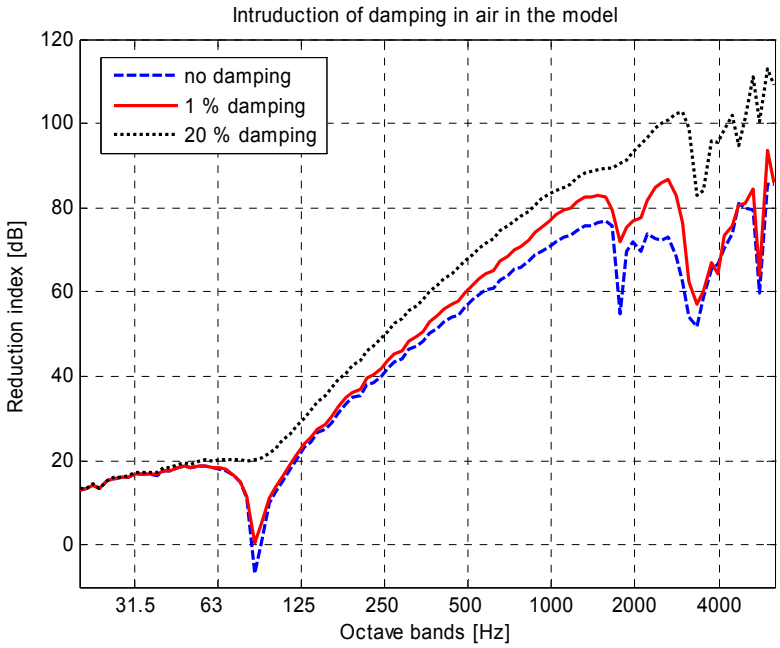

Figure 5.10: *Result of the (air) damping influence in the model. Calculations performed on a 10 meter wide wall between 20 and 6000 Hertz.*

Also the overall reduction index is increased when there is damping in the model which is natural when the wavelength comes closer to the distance between the plates. (Higher frequencies are damped more than lower.)

Now when we know that the damping is correctly introduced in the model it is harder to explain the values in the parameter study. A reason for that the reduction index for all the walls with damping are the same, could be that one has to go higher in frequency to see a difference. The frequency is too low to have many wavelengths fit between the plates or studs. If different damping values are investigated over a large distance at high frequency, the differences would be visible. In figure 5.10 above, the damping effect is easily seen because there are no studs and, the model is 10 meters wide instead of the default 3 meters. I.e. it has a much larger continuous air space. Another reason for the result in figure 5.9 could be that the sound bridges the studs create are so dominant when it comes to sound transmission that, an increase in air-damping does not affect the reduction index much.

5.2. Comparison with results from an earlier study

Why the study of unequally stiff plates was made, is because of the results Haike showed in her paper. Some of the chosen values of the Young's modulus fall within the criterions that were set up by Brick [1]. She states that a decrease in radiation efficiency can be seen when a discontinuous coupling pattern (between the plates) is used instead of a continuous. A summary of the criterion is that the resonance frequency of the air coupling has to be lower than the critical frequency of plate 1 and, the critical frequency of plate 1 has to be lower than the resonance frequency of the studs. Further the critical frequency of plate 2 has to be higher than the resonance frequency of the studs. (See also figure 5.11.)

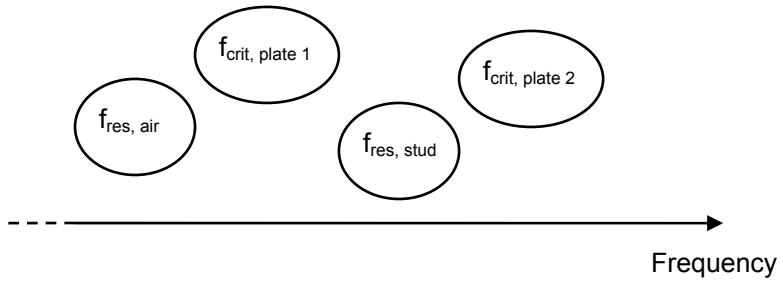

Figure 5.11: *Interpretation of the criterions that Brick presented in her report. [1]*

A calculation, using Brick's model for radiated power, of two continuously coupled and two discontinuously coupled plates was performed. The plates and interlayer have properties that meet the above mentioned criterions and, the result of the calculation can be seen in figure 5.12. Note the difference in radiated power above the first resonances of the structure.

To see if the reduction index would behave the same way, a FEM-calculation of the exact same structure was made. One stiff (aluminum) and one soft (lead) plate were used and the coupling material (Sylomer V12 and air) was modeled as mass-less in order to get good conformity with Brick's results. Note, when comparing figures 5.12 and 5.13, that the radiated power and the reduction index are inversely proportional.

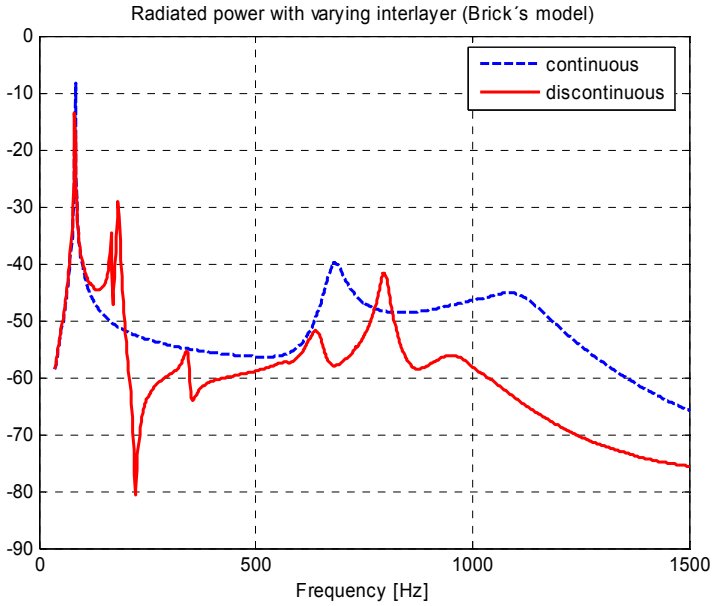

Figure 5.12: *Result from calculation of radiated power, using Brick's model.*

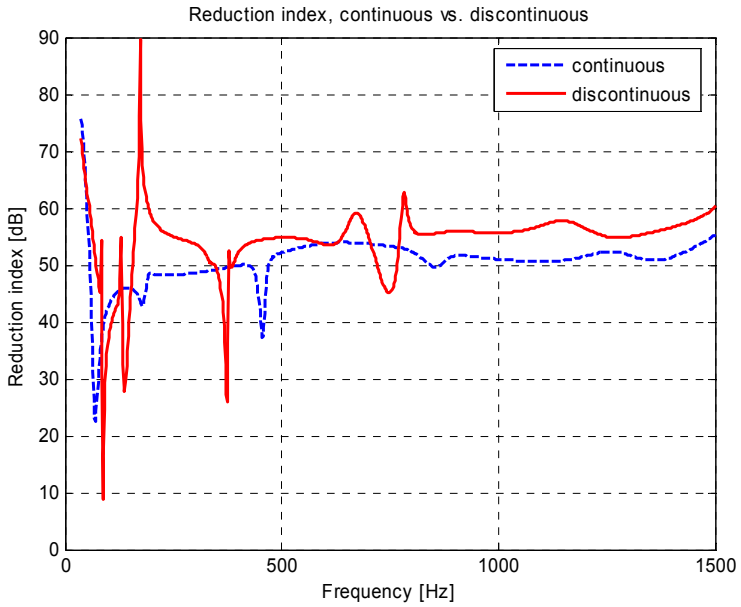

Figure 5.13: *Result from the FEM-calculation of the reduction index.*

The graph shows an approximate increase of 6 dB in reduction index at higher frequencies, when using a discontinuous coupling pattern rather than a continuous. To get an understanding of the reason for this effect, the displacement of the structures has been plotted at 1000 Hertz. (See figures 5.14 and 5.15.)

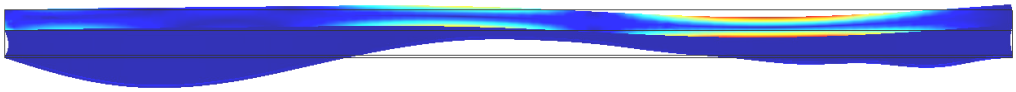

Figure 5.14: *Displacement of the continuously coupled plates at 1000 Hertz. A plane sound wave hits the structure from above, at an incident angle of 45 degrees.*

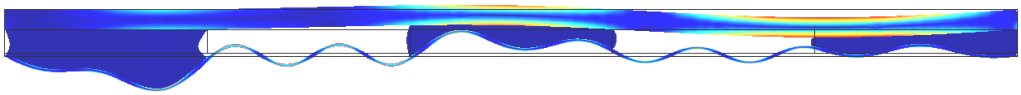

Figure 5.15: *Displacement of the discontinuously coupled plates at 1000 Hertz. A plane sound wave hits the structure from above, at an incident angle of 45 degrees.*

The wavelength and vibration pattern of the upper and lower plate of the continuously coupled structure is similar, while for the discontinuous case this is not true. Hence, the reduction of the sound is increased for the discontinuously coupled plates.

6.Discussion

6.1. Theory

The theory behind the reduction index is well developed when it comes to strict geometries such as walls consisting of a single plate or two parallel plates with only air between. But, when the structures become more complex, there is no general approach that works any more. This could be a reason for that well known constructions of walls mostly are used. These walls have well defined reduction indices, based on data collected both from theory and measurements. Although the building industry seems to be rather conservative, there would be an interest in new constructions that reduce sound in a cost efficient way. Therefore, a more detailed theory is needed to investigate this matter.

6.2. Model

The reduction index model presented in this report could be one way to do an inexpensive and time efficient investigation on how to increase the reduction index of a structure. The model is assumed to give approximately the same result as a measurement would of a specific structure but since in finite element programs, material properties are easily changed which is an advantage over doing measurements. If for example the influence on reduction index from bending stiffness of the studs should be investigated by measurements, one wall for each parameter has to be built. That is impossible to do without (unknowingly) doing any other modifications on the wall than the desired. Therefore, in this case a computer model is superior.

The limitation to 2D in the model does not seem to give incorrect results. Even though the first reason to limit it to 2D was because of the calculation time. One has to have in mind that there is one vibration pattern to calculate for each frequency and incident angle of the plane wave hitting the structure. (In the parameter study, 30 incident angles and 100 frequencies are considered which gives 3,000 different vibration patterns and, each of the 3000 calculations has approximately 45,000 degrees of freedom.) Looking at the result from a calculation of a double wall and comparing it to a hand calculation (see chapter 4.2) they seem to have a good agreement even though the hand calculation is based on 3D theory.

The model gives of course not a perfect representation of reality and, there are still some modifications that could improve its efficiency. In the model, the plates are perfectly glued to the studs and in reality there is total connection only where the screws (or nails, etcetera) are placed. This point connection could possible be implemented in the model. Modifications could also be done on the plates alone. A plate in the model consists of one large plate but in reality, for example gypsum boards are used and they are smaller than regular walls. It means that several boards have to be placed side by side in order to represent one plate in the model. The result is that waves could travel easier in the model plate than from one board to the other in reality. The difference in vibration pattern will be seen in the low frequency region. Modifications of this sort could be implemented in the model but there is no reason to make it more complex since it is impossible to mimic reality perfectly anyway. Naturally the model should be as close to reality as possible but it is always a matter of computer resources and calculation times.

6.3. Parameter study

The parameter study was performed on a wall structure that measured 3 meters in length. This length was chosen so that the first resonance of the whole structure would be lower in frequency than the double wall resonance since, below the first resonance the reduction index is stiffness controlled. If the double wall resonance would be in the stiffness controlled region it would not be seen as a dip in the reduction index.

The parameters that were changed were chosen because they, intuitively, have the most influence on the reduction index. Also the stiffness dependence Brick [1] found out had influence on the choice of parameters. The study could of course include many more parameters but that reaches beyond the scope of this report.

7.Summary & conclusions

7.1. Model

The construction of a complex computer model in order to find out the reduction index of an arbitrary structure is possible. The results agree well with earlier calculation models for single and double leaf structures. A draw back is that a full calculation (high frequency resolution over a large frequency span) requires a lot of computer resources but, the computer industry produces faster computers every year. With today's computers, a detailed investigation in a specific frequency region can be done in a few minutes, for example a closer look at the double wall resonance.

In the model, a finite element calculation is used in order to determine the vibration pattern of the structure in question, due to a sound pressure load acting on it. The finite element method is constructed to give the displacement in discrete points of the structure. The number and location of the points are determined by the so-called mesh, whose resolution is determined by the wavelength of the vibrations in the air and structure. Six discrete points for each wavelength is enough to reconstruct the correct vibration pattern. When the vibrations of the radiating side of the structure are known, the pressure it creates can be calculated by the Rayleigh integral. Because the added power on the structure is known, the reduction index can be determined for the calculated frequencies.

The model is limited to 2D in order to keep calculation time down. Since the length of possible studs in a wall usually is much longer than their width and height, this is a reasonable approximation. A modification of the model could be to calculate the vibrations in the 3D-domain but, when the calculated result is compared with the hand calculation method (see chapter 4.2) a good agreement can be seen. Since that the method agrees well with measurements of double walls with no studs [6], the conclusion that the calculation model presented in this paper also agrees with measurements, is drawn. This is also an argument to limit the model to two dimensions.

7.2. Parameter study

The parameter study shows both results that can verify the model and also results that correspond well with earlier results [1]. A verification of the model is easily seen when changing the density of the plates in a double wall with studs. An increase in density will lead to an increate in reduction index. Results that verify an earlier study is when the Young's modulus of the two plates is changed individually (resulting in different bending stiffness of the plates). The reduction index can be increased by using plates with different Young's modulus, making them vibrate with different patterns more easy. To obtain different vibration patterns is one aim when trying to increase the reduction index. (This makes the difference in reduction index between single leaf and double leaf constructions.)

7.3. Future work

Modifications of the model could also be of interest. Another FEM program that allows infinite structures could be used to exclude the boundary effects at low frequencies. An extension into 3D could be of interest if the coupling between the plates does not consist of infinite studs but, of solids that are finite in all directions (for example a rubber cube). At least at low frequencies this would be possible.

A well controlled measurement could be done in order to validate the calculation model. Especially a wall with studs since the validation done in this work is only of a wall with no studs. (See chapter 4.2.)

Optimization of a wall structure, both in a geometrical point of view and in a material property point of view. Then to realize such wall with reasonable building materials if possible.

Bibliography

[1] **H. Brick**, *Vibration behaviour of discontinuously coupled plates*, Diploma Thesis, Sept. 16th 2000, Institute for Technical Acoustics, Berlin, Germany & Department of Applied Acoustics, Göteborg, Sweden.

[2] **L. Cremer & M. Heckl**, *Structure – Bourne Sound*, Springer-Verlag, Berlin, 1973.

[3] **F. Fahy**, *Sound and Structural Vibration*, Academic Press, London, 1985.

[4] **M. Heckl**, *Journal of Sound and Vibration* (1981) 77(2), 165-189.

[5] **A. Tadeu**, *Applied Acoustics* 65 (2004), 15-29.

[6] **T.E. Vigran,** *Bygningsakustikk – ett grunnlag*, Tapir Akademisk Forlag, Trondheim, 2002.

Appendix

Below is the MatLab®/FEMLab® code from part of the parameter study presented. There is one main program (`tot_calc_adpmesh`) where the frequency vector, incident angle vector and some material data is specified. The program calls two sub-programs (`default_studs` & `W_calc`) where the velocity of the radiating boundary is calculated by FEMLab® and input and output power calculated from the obtained velocities. Finally, the reduction index is calculated in the main program.

```
function [f_tot,R_tot]=tot_calc_adpmesh;

%%%%%%%%%%%%%%%%%%%%%%%%%%%%%%%%%%%%%%%%%%%%%%%%%%%%%%%%%%%%%%%%%%%%%%%%%%%%%%%%
%                                                                               %
%   Reduction index calculation, using finite elements                          %
%                                                                               %
%   Developed by: Morten Lindborg                                               %
%                 Department of Civil and Environmental Engineering             %
%                 Division of Applied Acoustics                                 %
%                 CHALMERS UINIVERSITY OF TECHNOLOGY                            %
%                 Göteborg, Sweden 2005                                         %
%                                                                               %
%%%%%%%%%%%%%%%%%%%%%%%%%%%%%%%%%%%%%%%%%%%%%%%%%%%%%%%%%%%%%%%%%%%%%%%%%%%%%%%%

global ang f velo max_mesh E h rho

disp('Start time:')
disp(num2str(clock))
t0=clock;

% Material data
% ------
% Air
c=343;      % Speed of sound

% Plates
E=1e9;      % Youns's modulus of the plates
h=0.013;    % Thickness
rho=800;    % Density
% ------

% Which angel/-s to calculate:
% ------
ang=linspace(1,90,30);
% ------

% Which frequency/-ies to calculate:
% ------
f_tot=logspace(1.3,3.8,100);
% ------
```

```
for ff=1:length(f_tot);

f=f_tot(ff);

% Mesh size (Adaption for a optimal mesh is done for each frequency.)
% ------
% Wavelength calculation in the air and in the plate
lambda=c/f;
lambda_B=sqrt(sqrt(E*h^2*pi^2/(3*rho))/f);

% The dominating wavelength is chosen
max_mesh=min(lambda/6,lambda_B/6);
% ------


% Which femlab model to use:
% ------
[velo]=default_studs(max_mesh,ang,f); %SUB-PROGRAM!
% ------

% Calculation of input and output power
% ------
[W_in,W_out]=W_calc(velo,ang,f); %SUB-PROGRAM!
% ------

% Reduction index calculation
% ------
delta_ang=90/length(ang);

W_in_tot(ff)=2*delta_ang*pi/180*sum(W_in,1);
W_out_tot(ff)=2*delta_ang*pi/180*sum(W_out,1);

Tau_tot(ff)=W_out_tot(ff)/W_in_tot(ff);

R_tot(ff)=10*log10(1./Tau_tot(ff));
% ------

end


disp('Total calculation time (min):')
disp(etime(clock,t0)/60)
disp('Finish time:')
disp(num2str(clock))
```

```
function [velo]=default_studs(max_mesh,ang,f);

% FEMLab-calculation of the vibration of the structure:

flclear fem

% Femlab version
clear vrsn
vrsn.name = 'FEMLAB 3.0';
vrsn.ext = 'a';
vrsn.major = 0;
vrsn.build = 228;
vrsn.rcs = '$Name:  $';
vrsn.date = '$Date: 2004/04/05 18:04:31 $';
fem.version = vrsn;


% Geometry

% Plates:
g1=rect2('3','h','base','corner','pos',{'0','0.113'},'rot','0');
g2=rect2('3','h','base','corner','pos',{'0','0'},'rot','0');

% End studs:
g3=rect2('0.02','0.1','base','corner','pos',{'0','0.013'},'rot','0');
g4=rect2('0.02','0.1','base','corner','pos',{'2.98','0.013'},'rot','0')
;

% Studs:
g5=rect2('0.04','0.1','base','center','pos',{'0.6','0.063'},'rot','0');
g6=rect2('0.04','0.1','base','center','pos',{'1.2','0.063'},'rot','0');
g7=rect2('0.04','0.1','base','center','pos',{'1.8','0.063'},'rot','0');
g8=rect2('0.04','0.1','base','center','pos',{'2.4','0.063'},'rot','0');

% Air cavities:
g9=rect2('0.56','0.1','base','corner','pos',{'0.02','0.013'},'rot','0')
;
g10=rect2('0.56','0.1','base','corner','pos',{'0.62','0.013'},'rot','0'
);
g11=rect2('0.56','0.1','base','corner','pos',{'1.22','0.013'},'rot','0'
);
g12=rect2('0.56','0.1','base','corner','pos',{'1.82','0.013'},'rot','0'
);
g13=rect2('0.56','0.1','base','corner','pos',{'2.42','0.013'},'rot','0'
);

clear s
s.objs={g2,g5,g6,g7,g8,g4,g3,g1,g9,g10,g11,g12,g13};
s.name={'P2','S1','S2','S3','S4','SB','SA','P1','A1','A2','A3','A4','A5
'};
s.tags={'g2','g4','g5','g6','g7','g8','g3','g1','g9','g10','g11','g12',
'g13'};

fem.draw=struct('s',s);
fem.geom=geomcsg(fem);
```

```
% Initialize mesh
fem.mesh=meshinit(fem, ...
                  'hmax',[max_mesh], ...%   <--- MESH
                  'hmaxfact',1, ...
                  'hgrad',1.3, ...
                  'hcurve',0.3, ...
                  'hcutoff',0.001, ...
                  'hnarrow',1, ...
                  'hpnt',10, ...
                  'xscale',1.0, ...
                  'yscale',1.0);


% Application mode 1 (Plain strain)
clear appl
appl.mode.class = 'SmePlaneStrain';
appl.mode.type = 'cartesian';
appl.dim = {'u','v','u_t','v_t'};
appl.sdim = {'x','y','z'};
appl.name = 'pn';
appl.shape = {'shlag(2,''u'')','shlag(2,''v'')'};
appl.sshape = 2;
appl.border = 'off';
appl.assignsuffix = '_pn';
appl.assign =
{'Ex','Ex_pn','Ey','Ey_pn','Ez','Ez_pn','Fx','Fx_pn','FxAmp','FxAmp_p
n','FxPh','FxPh_pn','Fxg','Fxg_pn','Fy','Fy_pn','FyAmp','FyAmp_pn','F
yPh','FyPh_pn','Fyg','Fyg_pn','Gxy','Gxy_pn','Tax','Tax_pn','Tax_amp'
,'Tax_amp_pn','Tax_ph','Tax_ph_pn','Tay','Tay_pn','Tay_amp','Tay_amp_
pn','Tay_ph','Tay_ph_pn','alphax','alphax_pn','alphay','alphay_pn','a
lphaz','alphaz_pn','ex','ex_pn','ex_amp','ex_amp_pn','ex_ph','ex_ph_p
n','exi','exi_pn','exy','exy_pn','exy_amp','exy_amp_pn','exy_ph','exy
_ph_pn','exyi','exyi_pn','ey','ey_pn','ey_amp','ey_amp_pn','ey_ph','e
y_ph_pn','eyi','eyi_pn','ezi','ezi_pn','nuxy','nuxy_pn','nuxz','nuxz_
pn','nuyz','nuyz_pn','sx','sx_pn','sx_amp','sx_amp_pn','sx_ph','sx_ph
_pn','sxi','sxi_pn','sxy','sxy_pn','sxy_amp','sxy_amp_pn','sxy_ph','s
xy_ph_pn','sxyi','sxyi_pn','sy','sy_pn','sy_amp','sy_amp_pn','sy_ph',
'sy_ph_pn','syi','syi_pn','sz','sz_pn','sz_amp','sz_amp_pn','sz_ph','
sz_ph_pn','szi','szi_pn'};
clear prop
prop.elemdefault='Lag2';
prop.analysis='freq';
prop.largedef='off';
prop.impl='weak';
prop.eigtype='freq';
prop.weakconstr=struct('value',{'off'},'dim',{{'lm1','lm2','lm3','lm4
'}});
appl.prop = prop;
clear pnt
pnt.Fx = {'0'};
pnt.FxAmp = {'1'};
pnt.FxPh = {'0'};
pnt.Fy = {'0'};
pnt.FyAmp = {'1'};
pnt.FyPh = {'0'};
pnt.loadcoord = {'global'};
pnt.constrcoord = {'global'};
pnt.constrtype = {'standard'};
pnt.H = {{'0','0';'0','0'}};
```

```
pnt.R = {{'0';'0'}};
pnt.Rx = {'0'};
pnt.Hx = {'0'};
pnt.Ry = {'0'};
pnt.Hy = {'0'};
pnt.ind = [1,1,1,1,1,1,1,1,1,1,1,1,1,1,1,1,1,1,1,1,1,1,1,1,1,1,1,1,1];
appl.pnt = pnt;
clear bnd
bnd.Fx = {'0','0','0','0','0','-p','p'};
bnd.FxAmp = {'1','1','1','1','1','1','1'};
bnd.FxPh = {'0','0','0','0','0','0','0'};
bnd.Fy = {'0','0','-2*exp(i*k*cos(theta*pi/180)*x)','p','-
p','0','0'};
bnd.FyAmp = {'1','1','1','1','1','1','1'};
bnd.FyPh = {'0','0','0','0','0','0','0'};
bnd.loadcoord =
{'global','global','global','global','global','global','global'};
bnd.loadtype = {'area','area','area','area','area','area','area'};
bnd.constrcoord =
{'global','global','global','global','global','global','global'};
bnd.constrtype =
{'standard','standard','standard','standard','standard','standard','s
tandard'};
bnd.H =
{{'0','0';'0','0'},{'0','0';'0','0'},{'0','0';'0','0'},{'0','0';'0','
0'},{'0','0';'0','0'},{'0','0';'0','0'},{'0','0';'0','0'}};
bnd.R =
{{'0';'0'},{'0';'0'},{'0';'0'},{'0';'0'},{'0';'0'},{'0';'0'},{'0';'0'
}};
bnd.Rx = {'0','0','0','0','0','0','0'};
bnd.Hx = {'0','1','0','0','0','0','0'};
bnd.Ry = {'0','0','0','0','0','0','0'};
bnd.Hy = {'0','1','0','0','0','0','0'};
bnd.ind =
[2,1,1,1,2,1,3,6,5,4,7,1,1,6,5,4,7,1,1,6,5,4,7,1,1,6,5,4,7,1,1,6,5,4,
7,1,1,2,1,2];
appl.bnd = bnd;
clear equ
equ.shape = {[1;2],[1;2],[1;2]};
equ.gporder = {{4;4},{4;4},{4;4}};
equ.cporder = {{2;2},{2;2},{2;2}};
equ.init = {{'0';'0';'0';'0'},{'0';'0';'0';'0'},{'0';'0';'0';'0'}};
equ.usage = {0,1,1};
equ.E = {'2.0e11','E','1e10'};%  <--- E-mods
('"air"','plate','studs')
equ.rho = {'7850','rho','500'};%   <--- Densities
('"air"','plate','studs')
equ.alphadM = {'1','0','0'};
equ.betadK = {'0.001','0.02/omega','0.02/omega'};%   <--- Damping
('"air"','plate','studs')
equ.materialcoord = {'global','global','global'};
equ.materialmodel = {'iso','iso','iso'};
equ.hardeningmodel = {'iso','iso','iso'};
equ.yieldtype = {'mises','mises','mises'};
equ.isodata = {'tangent','tangent','tangent'};
equ.ETkin = {'2.0e10','2.0e10','2.0e10'};
equ.ETiso = {'2.0e10','2.0e10','2.0e10'};
equ.Sys = {'2.0e8','2.0e8','2.0e8'};
equ.Syfunc = {'mises_pn','mises_pn','mises_pn'};
```

```
equ.Syfunc_kin = {'misesKin_pn','misesKin_pn','misesKin_pn'};
equ.Shard = {'2.0e10/(1-2.0e10/2.0e11)*epe_pn','2.0e10/(1-
2.0e10/2.0e11)*epe_pn','2.0e10/(1-2.0e10/2.0e11)*epe_pn'};
equ.ini_stress = {'0','0','0'};
equ.ini_strain = {'0','0','0'};
equ.sxyi = {'0','0','0'};
equ.exyi = {'0','0','0'};
equ.sxi = {'0','0','0'};
equ.exi = {'0','0','0'};
equ.syi = {'0','0','0'};
equ.eyi = {'0','0','0'};
equ.szi = {'0','0','0'};
equ.ezi = {'0','0','0'};
equ.alpha = {'1.2e-5','1.2e-5','1.2e-5'};
equ.nu = {'0.33','0.35','0.35'};
equ.Gxy = {'7.52e10','7.52e10','7.52e10'};
equ.nuxy = {'0.33','0.33','0.33'};
equ.alphax = {'1.2e-5','1.2e-5','1.2e-5'};
equ.Ex = {'2.0e11','2.0e11','2.0e11'};
equ.nuyz = {'0.33','0.33','0.33'};
equ.alphay = {'1.2e-5','1.2e-5','1.2e-5'};
equ.Ey = {'2.0e11','2.0e11','2.0e11'};
equ.nuxz = {'0.33','0.33','0.33'};
equ.alphaz = {'1.2e-5','1.2e-5','1.2e-5'};
equ.Ez = {'2.0e11','2.0e11','2.0e11'};
equ.D = {{'2.0e11/((1+0.33)*(1-2*0.33))*(1-
0.33)','2.0e11/((1+0.33)*(1-2*0.33))*0.33','2.0e11/((1+0.33)*(1-
2*0.33))*0.33','0';'2.0e11/((1+0.33)*(1-
2*0.33))*0.33','2.0e11/((1+0.33)*(1-2*0.33))*(1-
0.33)','2.0e11/((1+0.33)*(1-2*0.33))*0.33','0';'2.0e11/((1+0.33)*(1-
2*0.33))*0.33','2.0e11/((1+0.33)*(1-
2*0.33))*0.33','2.0e11/((1+0.33)*(1-2*0.33))*(1-
0.33)','0';'0','0','0','2.0e11/((1+0.33)*2)'},{'2.0e11/((1+0.33)*(1-
2*0.33))*(1-0.33)','2.0e11/((1+0.33)*(1-
2*0.33))*0.33','2.0e11/((1+0.33)*(1-
2*0.33))*0.33','0';'2.0e11/((1+0.33)*(1-
2*0.33))*0.33','2.0e11/((1+0.33)*(1-2*0.33))*(1-
0.33)','2.0e11/((1+0.33)*(1-2*0.33))*0.33','0';'2.0e11/((1+0.33)*(1-
2*0.33))*0.33','2.0e11/((1+0.33)*(1-
2*0.33))*0.33','2.0e11/((1+0.33)*(1-2*0.33))*(1-
0.33)','0';'0','0','0','2.0e11/((1+0.33)*2)'},{'2.0e11/((1+0.33)*(1-
2*0.33))*(1-0.33)','2.0e11/((1+0.33)*(1-
2*0.33))*0.33','2.0e11/((1+0.33)*(1-
2*0.33))*0.33','0';'2.0e11/((1+0.33)*(1-
2*0.33))*0.33','2.0e11/((1+0.33)*(1-2*0.33))*(1-
0.33)','2.0e11/((1+0.33)*(1-2*0.33))*0.33','0';'2.0e11/((1+0.33)*(1-
2*0.33))*0.33','2.0e11/((1+0.33)*(1-
2*0.33))*0.33','2.0e11/((1+0.33)*(1-2*0.33))*(1-
0.33)','0';'0','0','0','2.0e11/((1+0.33)*2)'}};
equ.alphavector = {{'1.2e-5';'1.2e-5';'1.2e-5';'0'},{'1.2e-5';'1.2e-
5';'1.2e-5';'0'},{'1.2e-5';'1.2e-5';'1.2e-5';'0'}};
equ.thickness = {'1','1','1'};
equ.Fx = {'0','0','0'};
equ.FxAmp = {'1','1','1'};
equ.FxPh = {'0','0','0'};
equ.Fy = {'0','0','0'};
equ.FyAmp = {'1','1','1'};
equ.FyPh = {'0','0','0'};
equ.loadcoord = {'global','global','global'};
```

```
equ.Tflag = {'0','0','0'};
equ.Temp = {'0','0','0'};
equ.Tempref = {'0','0','0'};
equ.loadtype = {'volume','volume','volume'};
equ.constrcoord = {'global','global','global'};
equ.constrtype = {'standard','standard','standard'};
equ.H = {{'0','0';'0','0'},{'0','0';'0','0'},{'0','0';'0','0'}};
equ.R = {{'0';'0'},{'0';'0'},{'0';'0'}};
equ.Rx = {'0','0','0'};
equ.Hx = {'0','0','0'};
equ.Ry = {'0','0','0'};
equ.Hy = {'0','0','0'};
equ.ind = [2,3,2,1,3,1,3,1,3,1,3,1,3];
appl.equ = equ;
appl.var = {'freq','freq'};
fem.appl{1} = appl;


% Application mode 2 (Acoustics)
clear appl
appl.mode.class = 'Acoustics';
appl.mode.type = 'cartesian';
appl.dim = {'p','p_t'};
appl.sdim = {'x','y','z'};
appl.name = 'aco';
appl.shape = {'shlag(2,''p'')'};
appl.sshape = 2;
appl.border = 'off';
appl.assignsuffix = '_aco';
clear prop
prop.elemdefault='Lag2';
prop.analysis='harmonic';
prop.weakconstr=struct('value',{'off'},'dim',{{'lm5','lm6'}});
appl.prop = prop;
clear bnd
bnd.p0 = {'0','0','0','0','0','0'};
bnd.Z =
{'1.25*343','1.25*343','1.25*343','1.25*343','1.25*343','1.25*343'};
bnd.nacc = {'0','0','-a_wall','a_wall','a_wood','-a_wood'};
bnd.x0 = {'0','0','0','0','0','0'};
bnd.y0 = {'0','0','0','0','0','0'};
bnd.qs0 =
{{'0';'0'},{'0';'0'},{'0';'0'},{'0';'0'},{'0';'0'},{'0';'0'}};
bnd.kdir = {{'-nx';'-ny'},{'-nx';'-ny'},{'-nx';'-ny'},{'-nx';'-
ny'},{'-nx';'-ny'},{'-nx';'-ny'}};
bnd.type = {'SS','cont','NA','NA','NA','NA'};
bnd.wavetype = {'PL','PL','PL','PL','PL','PL'};
bnd.ind =
[1,1,1,2,1,2,1,5,4,3,6,2,2,5,4,3,6,2,2,5,4,3,6,2,2,5,4,3,6,2,2,5,4,3,
6,2,2,1,1,1];
appl.bnd = bnd;
clear equ
equ.shape = {[1],[1]};
equ.gporder = {{4},{4}};
equ.cporder = {{2},{2}};
equ.init = {{'0';'0'},{'0';'0'}};
equ.usage = {1,0};
equ.rho = {'1.25','1.25'};
equ.cs = {'343','c'};%   <--- Speed of sound ('"structure"','air')
```

```
equ.qs = {{'0';'0'},{'0';'0'}};
equ.ind = [2,2,2,1,2,1,2,1,2,1,2,1,2];
appl.equ = equ;
appl.var = {'freq','freq','p_ref','20e-6'};
fem.appl{2} = appl;
fem.sdim = {'x','y'};

% Simplify expressions
fem.simplify = 'on';
fem.outform = 'weak';


% Boundary expressions
clear bnd
bnd.ind =
[1,1,1,1,1,1,1,1,1,1,1,1,1,1,1,1,1,1,1,1,1,1,1,1,1,1,1,1,1,1,1,1,1,
1,1,1,1,1,1,1];
bnd.dim = {'u','v','p'};
bnd.var = {};
bnd.expr = {'a_wall',{'-omega^2*v'},'a_wood',{'-omega^2*u'}};
fem.bnd = bnd;
fem.bnd = bnd;


% Loop for calculating the velocities of the radiating boundary for
% different incident angles.
% ------
for ii=1:length(ang);

% Global expressions
fem.expr = {'omega','2*pi*freq','k','2*pi*freq/343','theta',ang(ii)};

% Functions
fem.functions = {};

% Multiphysics
fem=multiphysics(fem);

% Extend mesh
fem.xmesh=meshextend(fem,'geoms',[1],'eqvars','on','cplbndeq','on','c
plbndsh','off');

% Solve problem
fem.sol=femlin(fem, ...
               'method','eliminate', ...
               'nullfun','flnullorth', ...
               'blocksize',5000, ...
               'complexfun','off', ...
               'conjugate','off', ...
               'symmetric','off', ...
               'solcomp',{'u','p','v'}, ...
               'outcomp',{'v'}, ...   % {'u','p','v'}
               'rowscale','on', ...
               'pname','freq', ...
               'plist',[f], ...
               'porder',1, ...
               'nonlin','off', ...
               'linsolver','umfpack', ...%   <--- FEM SOLVER
               'thresh',0.1, ...
```

```
                'umfalloc',1, ...%      <--- MEMORY ALLOCATION (0.1-1)
                'uscale','auto');

% Extraction of the velocity from the solution
v(ii)=posteval(fem,'v_t','cont','on','refine',1,'edim',1,...
    'dl',2,'solnum',[1:length(f)]);

end
% ------

% Save relevant data in one structure:
% ------
velo_data=zeros(length(v(1).p),length(f),length(v));

for ii=1:length(v);
    velo_data(:,:,ii)=[v(ii).d'];
end

x=v(1).p(1,:);

velo=struct('info',{'Point velocity for different freqs and angles,
velo.data=[points,freq,angle], velo.p=[point x-coord]'},...
    'data',velo_data,'p',x);
% ------
```

```
function [W_in,W_out]=W_calc(velo,ang,f);

% Calculation of the input and output power:

% Calculation of the distance from point on the plate to the
% points on the half sphere around the radiating plate
% ------
d=abs(velo.p(2)-velo.p(1));
mesh=length(velo.p);
r=10;
n=[1:mesh];
phi=pi/mesh*(n-1);
rho=1.21;
c=343;
delta_x=r*pi/mesh;

W_in=zeros(length(ang),length(f));
pnt_dist=zeros(mesh,mesh);
l=linspace(-velo.p(round(mesh/2)),velo.p(round(mesh/2+1)),mesh);

% The cosine law
for ii=1:length(phi);
    pnt_dist(ii,:)=sqrt(r^2+l.^2-2*r*l*cos(phi(ii)));
end
% ------

% Calculation of input power and, output power via the Rayleigh
integral
% ------
for rr=1:length(ang);

% Rayleigh
data_2=velo.data(:,:,rr);
p=zeros(mesh,length(f),mesh);

    for ii=1:mesh;
        Rm=pnt_dist(ii,:);
        for iii=1:length(f)
            k=2*pi*f(iii)/c;
            p(:,iii,ii)=2*pi*f(iii)*rho/2*data_2(ii,iii,1)*...
                (i/pi*sqrt(2*pi)./sqrt(k*Rm).*exp(-
i*(k*Rm+pi/4)))'*d;
        end
    end

p_pnt=sum(p,3); %pressure in each point with contribution from all
points

% Output power
W_out(rr,:)=delta_x/(1.21*343*2)*sum(abs(p_pnt).^2,1);

% Pressure on sending side
theta=ang(rr); %angle of insidence
k=2*pi*f/c;

p_send=zeros(length(velo.p),length(f));
for ii=1:length(velo.p);
    p_send(ii,:)=exp(i*k*cos(theta*pi/180)*velo.p(ii));
end
```

```
q=p_send/(rho*c)*d*sin(theta*pi/180); % flow velocity

% Input power
for ii=1:length(f);
    W_in(rr,ii)=abs(sum(0.5*real(p_send(:,ii).*conj(q(:,ii)))));
end

end
% ------
```
